Electronic Supplementary Material (ESI) for Nanoscale.

Supplementary information

Phospholipid-porphyrin conjugates: deciphering the driving forces behind their supramolecular assemblies

Louis-Gabriel Bronstein[1#], Ágota Tóth[2#], Paul Cressey[1], Véronique Rosilio[1], Florent Di Meo[2*] and Ali Makky[1*]

[1] *Université Paris-Saclay, CNRS, Institut Galien Paris-Saclay, 92296, Châtenay-Malabry, France*

[2] *INSERM U1248 Pharmacology & Transplantation, Univ. Limoges, 2 rue du Prof. Descottes, F-87025, Limoges, France*

[#] Equally contributed

[*] Corresponding authors: florent.di-meo@inserm.fr, ali.makky@universite.paris-saclay.fr

SUPPORTING MATERIALS CONTENTS

1. NMR characterization of BocNH-Gly-LPC

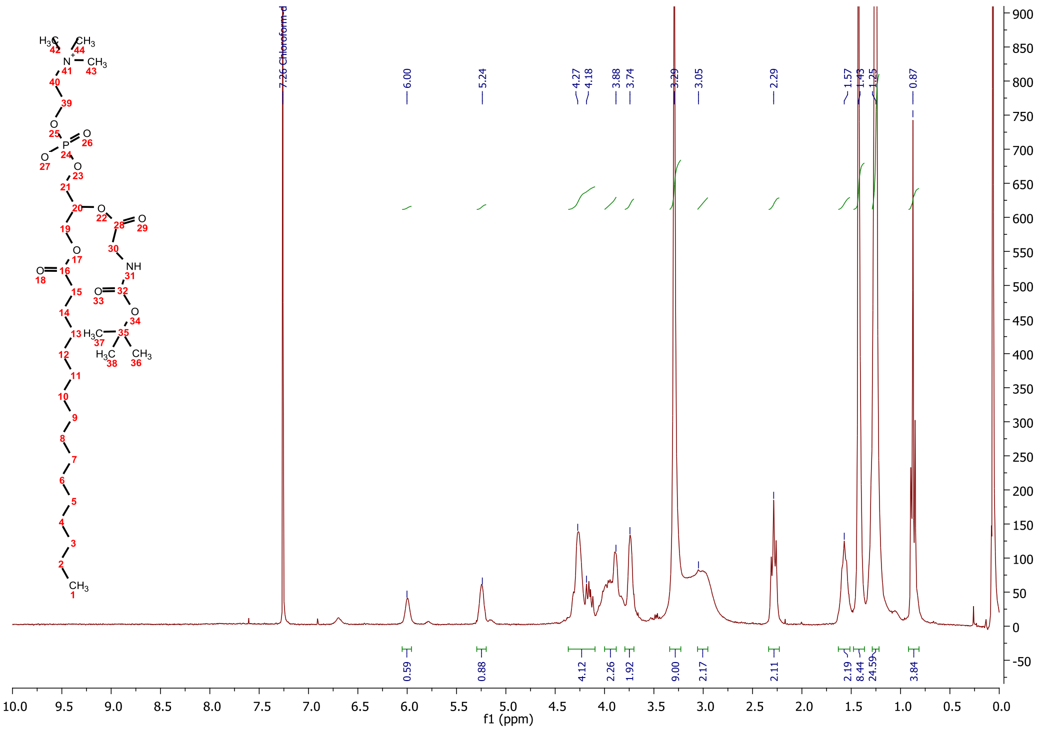

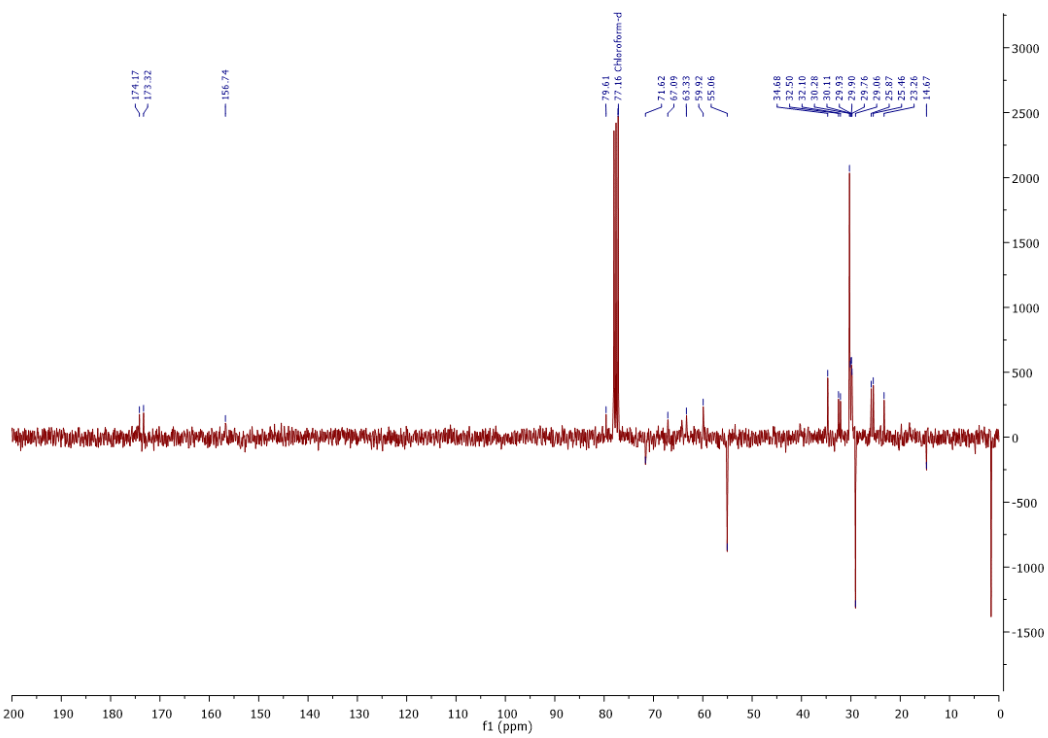

Figure S1. BocNH-Gly-LPC NMR details: ***^{1}H NMR*** *(300 MHz, $CDCl_3$) δ (ppm) = 5.89 (bs, 1H, NH), 5.25 (m, 1H, C_{20}), 4.28-4.17 (m, 4H, C_{40} & C_{19}), 4.07-3.83 (m, 2H, C_{21}), 3.74 (s, 2H, C_{39}), 3.36 (s, 9H, $C_{42\text{-}44}$), 3.05 (bs, 2H, C_{30}), 2.28 (t, 2H,J=7.5Hz, C_{15}), 1.55 (qu, 2H J=6.0 Hz, C_{14}), 1.42 (s, 9H, $C_{36\text{-}38}$), 1.25 (s, 24H, $C_{2\text{-}13}$), 0.87 (3H, t, J=6.9 Hz, C_1).* ***^{13}C NMR*** *(75 MHz, $CDCl_3$) δ = 174.17 (C=O), 173.32 (C=O), 156.74 (C=O), 79.61, 71.62 (CH), 67.09,* *63.33, 59.92, 55.06 ($N(CH_3)_3$), 34.68, 32.50, 32.10, 30.28, 30.11, 29.93, 29.90, 29.76, 29.06 ($C(CH_3)_3$), 25.87, 25.46, 23.26, 14.67(CH_3).*

2. NMR characterization of BocNH-Ala-LPC:

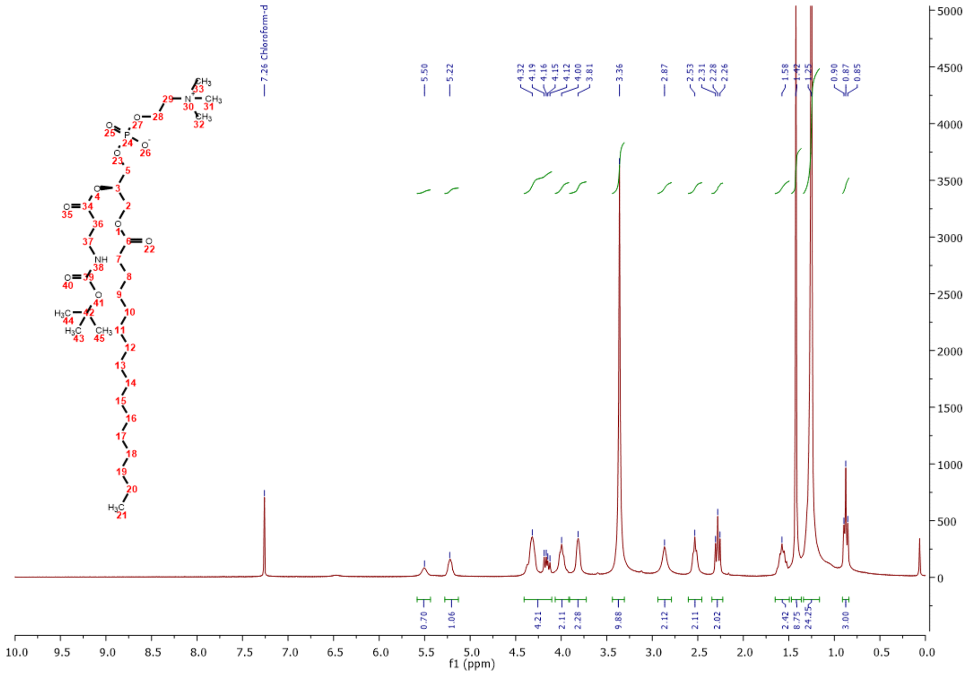

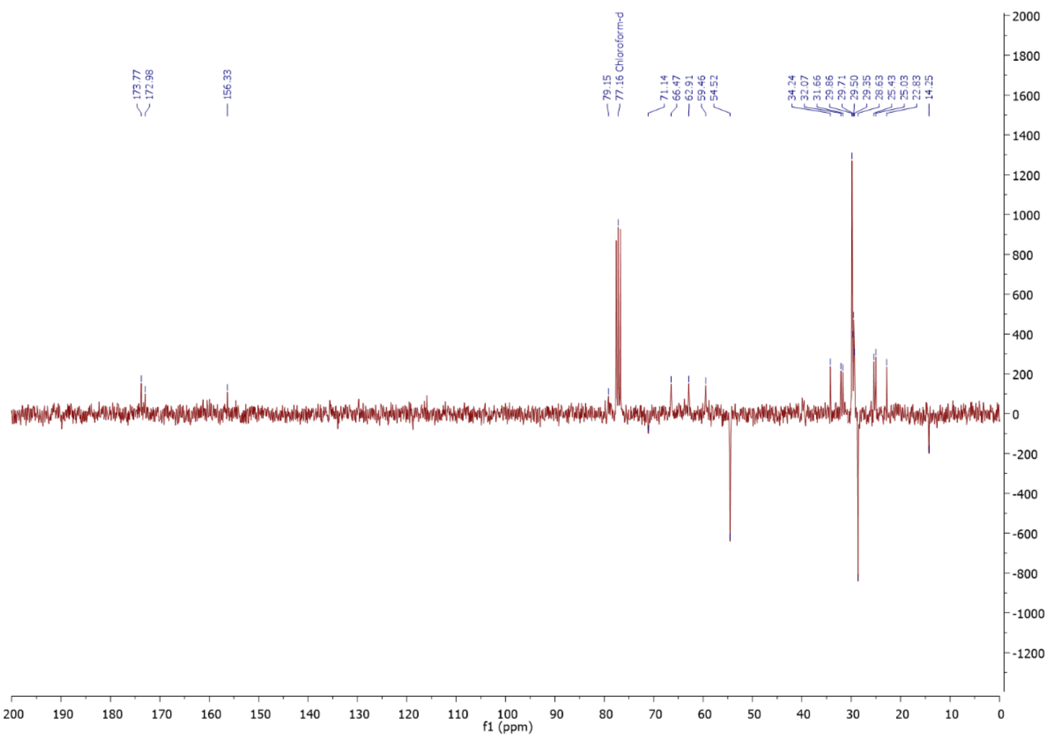

Figure S2. BocNH-Ala-LPC NMR details: ***^{1}H NMR*** *(300 MHz, $CDCl_3$) δ (ppm) = 5.51 (bs, 1H, NH), 5.21 (m, 1H, C_{20}), 4.32-4.16 (m, 4H, C_{40}-C_{19}), 4.06-3.94 (s, 2H, C_{21}), 3.81 (s, 2H, C_{39}), 3.36 (s, 9H, $C_{42\text{-}44}$), 2.86 (bs, 2H, C_{45}), 2.55 (t, 2H, J=6Hz,C_{30}), 2.28 (t, 2H, J=7.5Hz, C_{15}), 1.58 (qu, 2H,J= 6Hz, C_{14}), 1.42 (s, 9H, $C_{36\text{-}38}$), 1.25 (s, 24H, $C_{2\text{-}13}$), 0.87 (3H, t, C_1).* ***^{13}C NMR*** *(75 MHz, $CDCl_3$) δ = 173.77 (C=O), 172.98 (C=O), 156.33 (C=O), 79.15, 71.14 (CH), 66.47, 62.91, 59.46, 54.52 ($N(CH_3)_3$), 34.24, 32.07, 31.66, 29.86, 29.71, 29.50, 29.35, 28.63 ($C(CH_3)_3$), 25.43, 25.03, 22.83, 14.25 (CH_3).*

3. NMR characterization of BocNH-γBuA-LPC

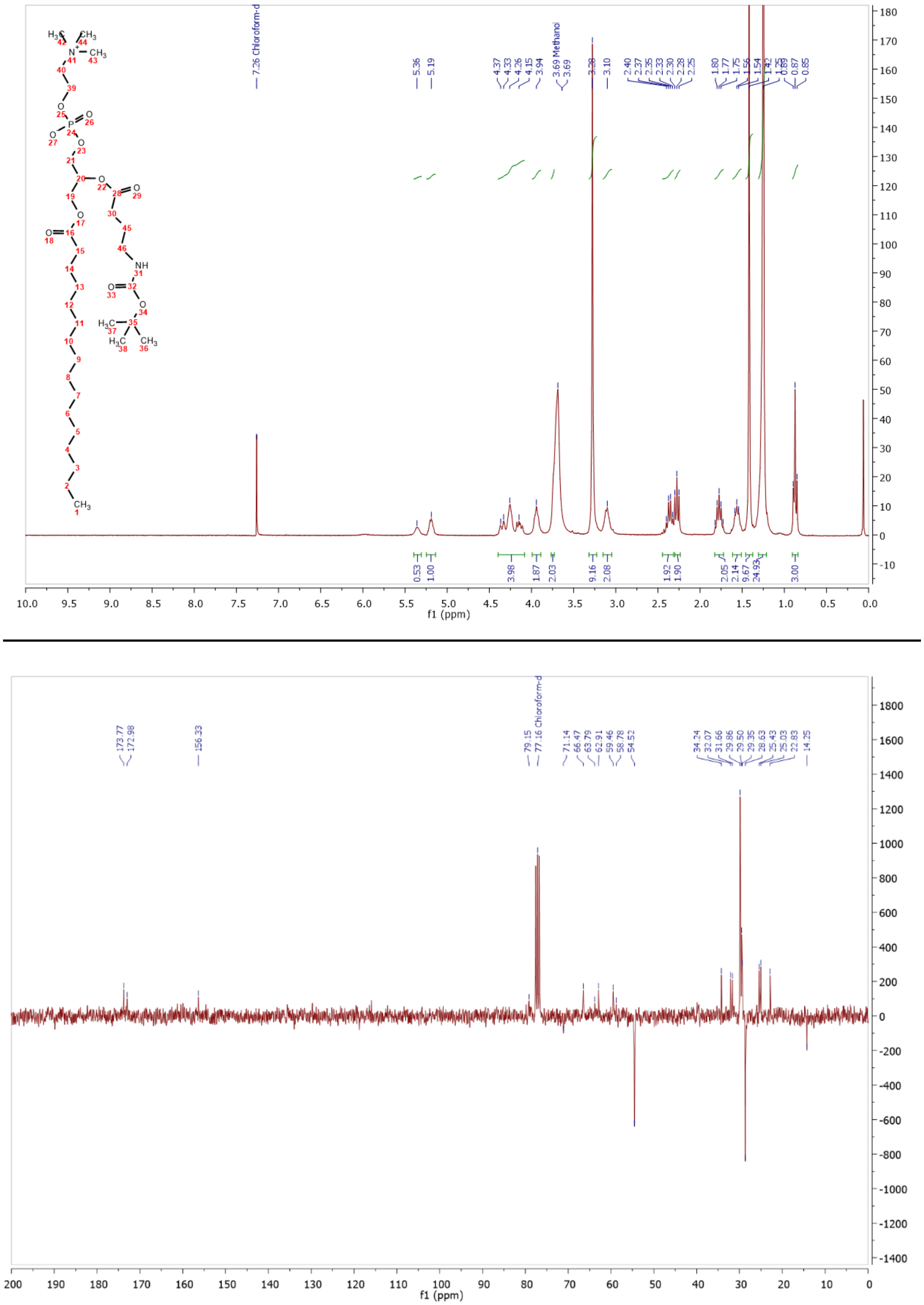

Figure S3. BocNH-γBuA-LPC NMR details: [1]***H NMR*** *(300 MHz, $CDCl_3$) δ (ppm) = 5.36 (bs, 1H, NH), 5.19 (m, 1H, C_{20}), 4.37-4.15 (m, 4H, C_{40}-C_{19}), 3.94 (m, 2H, C_{21}), 3.71 (m, 2H, C_{19}) 3.69 (MeOH), 3.28 (s, 9H, C_{42-44}), 3.10 (m, 2H, C_{46}), 2.37 (m, 2H, C_{30}), 2.28 (m, 2H, J=7.8Hz, C_{15}), 1.80 (qu, 2H, J=7.1Hz, C_{45}), 1.56 (m, 2H, C_{14}), 1.42 (s, 9H, C_{38-36}), 1.25 (s, 24H, C_{2-13}), 0.87 (t, 3H, C_1).* [13]***C NMR*** *(75 MHz, $CDCl_3$) δ = 173.77 (C=O), 172.98 (C=O), 156.33*

(C=O), 79.15, 71.14 (CH), 66.47, 63.79, 62.91, 59.46, 58.78, 54.52 ($N(CH_3)_3$), 34.24, 32.07, 31.66, 29.86, 29.50, 29.35, 28.63 ($C(CH_3)_3$), 25.43, 25.03, 22.83, 14.25 (CH_3).

4. NMR characterization of Ph_2LPC

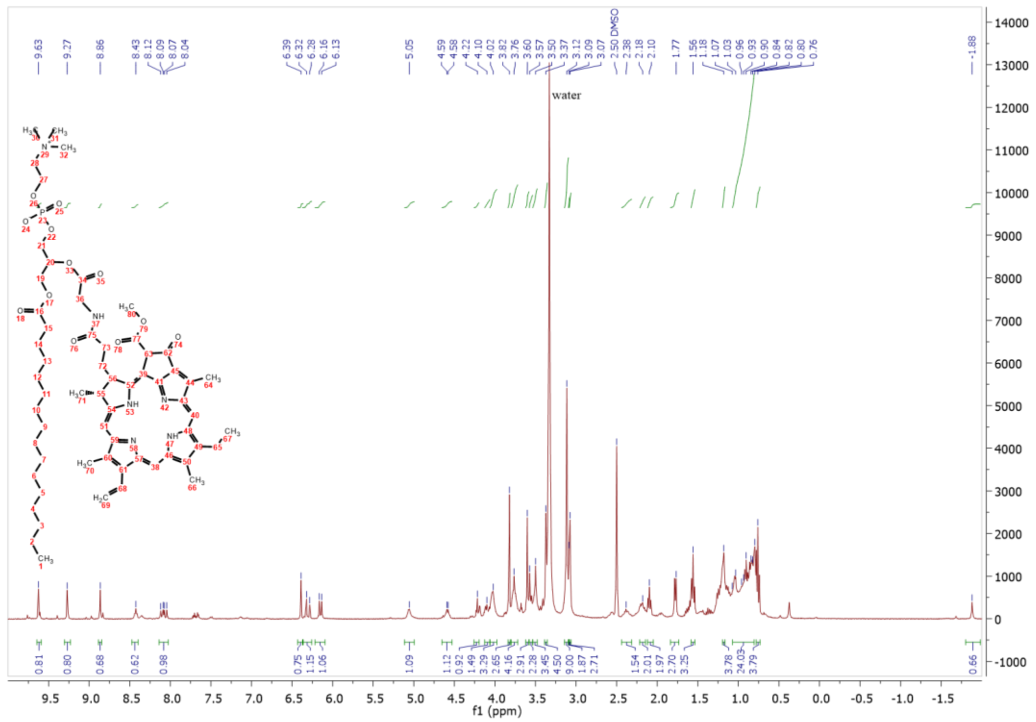

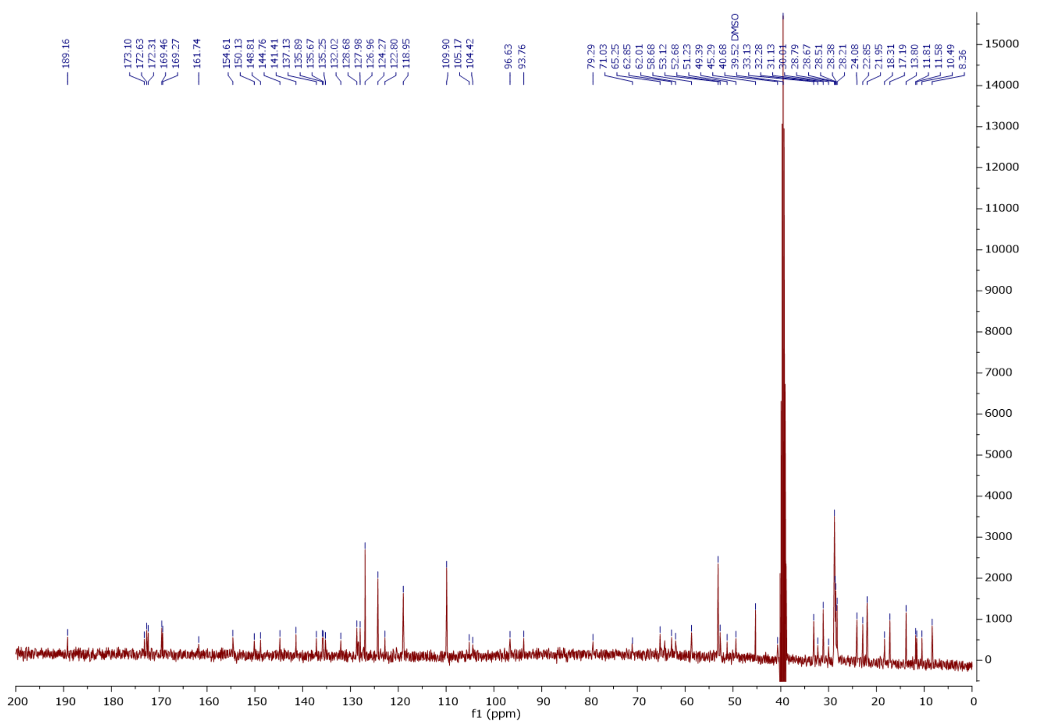

Figure S4. Ph_2LPC NMR details: ***^{1}H NMR*** *(400 MHz, DMSO-d_6) δ (ppm) = 9.63 (s, 1H, C_{38}), 9.27 (s, 1H, C_{40}), 8.86 (s, 1H, C_{51}), 8.43 (s, 1H, NH_{37}), 8.12-8.04 (dd, 1H, J=11.6-17.4 Hz, C_{68}), 6.39 (s, 1H, NH_{47}), 6.32-6.28 (d, 1H, J= 18Hz, C_{69}), 6.16-6.13 (d, 1H, J= 12Hz, C_{69}), 5.05 (m, 1H, C_{20}), 4.57 (m, 1H, C_{63}), 4.22 (m, 1H, C_{56}), 4.12 (m, 1H, C_{55}), 4.04 (m, 4H, C_{19}-C_{28}), 3.82 (s, 3H, C_{70}), 3.76 (m, 4H, C_{21}-C_{65}) , 3.60 (s, 3H, C_{64}), 3.57 (m, 2H, C_{27}), 3.37 (s, 3H,*

C_{66}), 3.12 (s, 9H, C_{30-32}), 3.09 (m, 2H, C_{36}), 3.07 (s, 3H, C_{80}), 2.37-2.19 (m, 4H, C_{72}-C_{73}), 2.10 (t, 2H, C_{15}), 1.78 (d, 3H, C_{71}), 1.56 (t, 3H, J= 7.1 Hz, C_{67}), 1.05-0.80 (m, 28H, C_{2-14}, C_{65}), 0.76 (t, 3H, J= 7.2 Hz, C_1), -1.9 (bs, 1H, NH_{53}). ***^{13}C NMR*** *(101 MHz, DMSO) δ = 189.16, 173.10, 172.63, 172.31, 169.46, 169.27, 161.74, 154.61, 150.13, 148.81, 144.76, 141.41, 137.13, 135.89, 135.67, 135.25, 132.02, 128.68, 127.98, 126.96, 124.27, 122.80, 118.95, 109.90, 105.17, 104.42, 96.63, 93.76, 79.29, 71.03, 65.25 ,64.28, 62.85, 62.01, 58.68, 53.12, 52.68, 51.23, 49.39, 45.29, 40.68, 39.52, 33.13, 32.28, 31.13, 30.01, 28.79, 28.67, 28.51, 28.38, 28.21, 24.08, 22.85, 21.95, 18.31, 17.19, 13.80, 11.81, 11.58, 10.49, 8.36.*

5. NMR characterization of Pyr$_2$LPC

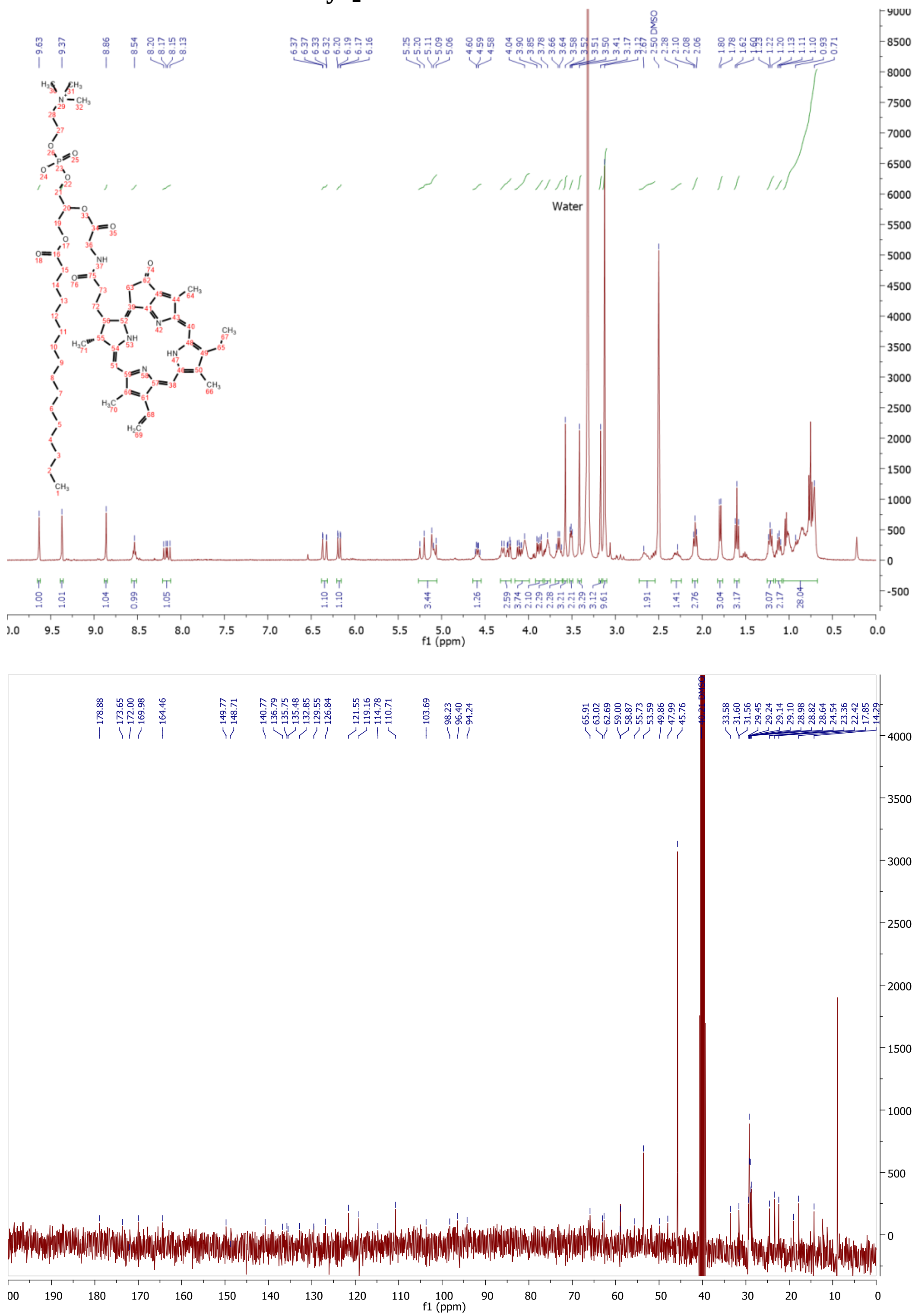

Figure S5. Pyr$_2$LPC NMR details: ***^{1}H NMR*** *(400 MHz , DMSO-d$_6$) δ (ppm) = 9.64 (s, 1H, C$_{38}$), 9.36 (s, 1H, C$_{40}$), 8.85 (s, 1H, C$_{51}$), 8.53 (m,1H, NH$_{37}$), 8.15 (dd, 1H, J=11.6-17.8 Hz, C$_{68}$), 6.34 (dd, 1H, J= 1.5-17.8 Hz, C$_{69}$), 6.17 (dd, 1H, 1.5-11.6 Hz, C$_{69}$), 5.25-5.03 (d ,1H, J=20 Hz, C$_{63}$), 5.11-5.06 (d, 1H, J= 20Hz, C$_{63}$), 5.03 (m, 1H, C$_{20}$), 4.58 (dt, 1H, C$_{56}$), 4.26 (m, 2H, C$_{21}$), 4.10 (dd, 1H, C$_{55}$), 4.04 (m, 2H, C$_{28}$), 3.86 (m, 2H, C$_{19}$), 3.77 (m, 2H, C$_{73}$), 3.66 (q,* *2H, C_{65}), 3.57 (s, 3H, C_{70}), 3.51 (m, 2H, C_{27}), 3.41 (s, 3H, C_{64}), 3.16 (s, 3H, C_{66}), 3.12 (s, 11H, C_{31-33}, C_{36}), 2.67 (m, 1H, C_{72}), 2.29 (m, 1H, C_{72}), 2.07 (t, 2H, C_{15}), 1.79 (d, 3H, C_{71}), 1.60 (t, 3H, C_{67}), 1.07-0.65 (m, 29H, C_{1-14}).* ***^{13}C NMR*** *(101 MHz, DMSO) δ = 200.80 (C=O), 178.88 (C=O), 173.65 (C=O), 172.00, 169.98, 164.46, 149.77, 148.71, 140.77, 136.79, 135.75, 135.48, 132.85, 129.55, 126.84, 121.55, 119.16, 114.78, 110.71, 103.69, 98.23, 96.40, 94.24, 65.91, 63.02, 62.69, 59.00, 58.87, 55.73, 53.59, 49.86, 47.99, 45.76, 33.58, 31.60, 31.56, 29.45, 29.24, 29.14, 29.10, 28.98, 28.82, 28.64, 24.54, 23.36, 22.42, 19.05, 17.85, 14.29.*

6. NMR characterization of Ph_3LPC

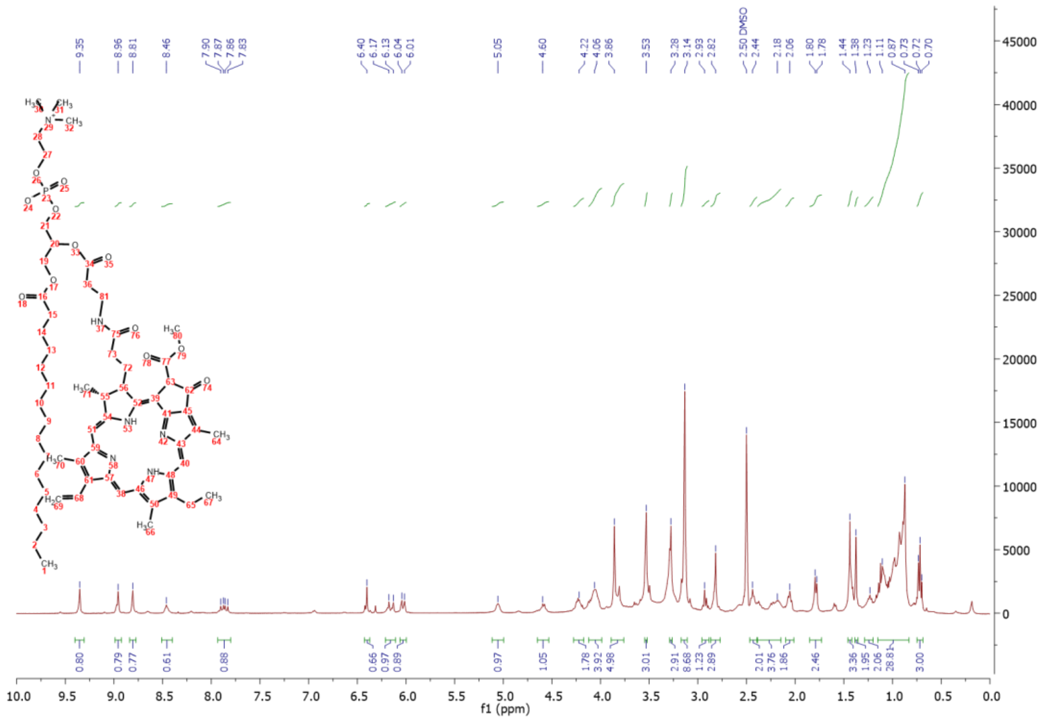

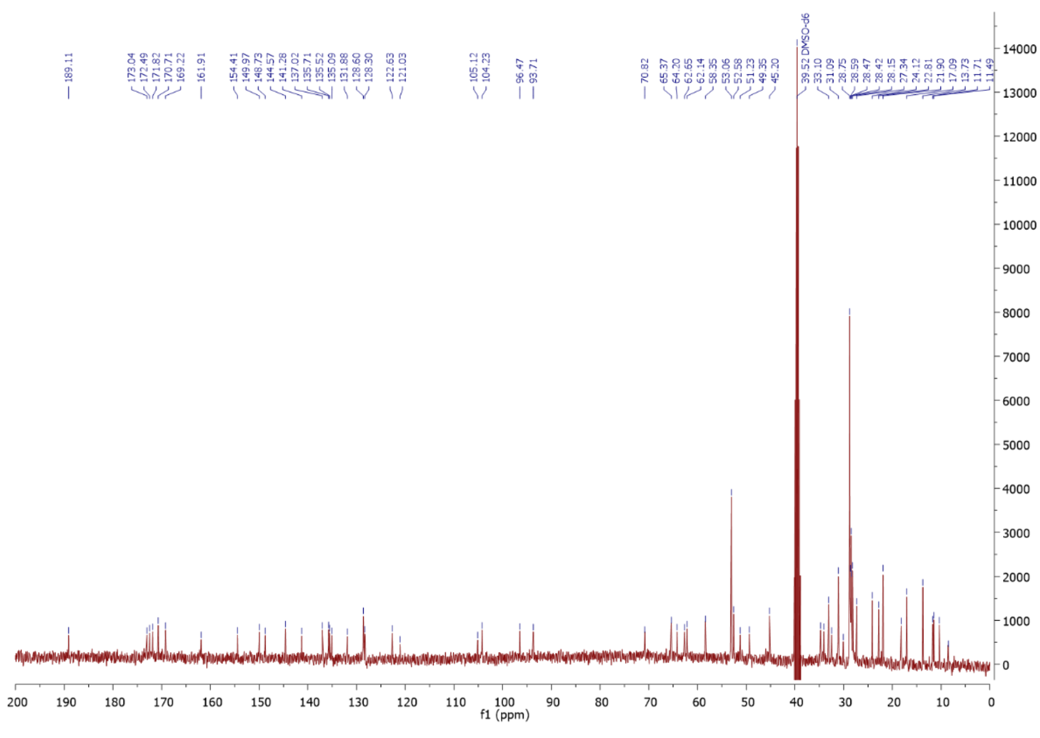

Figure S6. Ph_3LPC NMR details: ***[1]H NMR*** *(400 MHz, DMSO-d_6) δ (ppm) = 9.35 (s, 1H, C_{38}), 8.96 (s, 1H, C_{40}), 8.81 (s, 1H, C_{51}), 8.46 (s, 1H, NH_{37}), 7.87 (dd, 1H, J = 17.7-11.6 Hz, C_{68}), 6.4 (m, 1H, NH_{47}), 6.17-6.13 (dd, 1H, J = 1.5-18 Hz, C_{69}) , 6.04-6.01 (dd, 1H, J= 1.5-11.6 Hz, C_{69}), 5.05 (m, 1H, C_{20}), 4.60 (m, 1H, C_{63}), 4.22 (m, 2x1H, C_{55} - C_{56}), 4.06 (m, 4H, C_{19}-C_{28}), 3.86 (m, 5H, C_{70}-C_{21}), 3.53 (s, 5H, C_{64} – C_{65}), 3.28 (m, 5H, C_{66}, C_{27}), 3.14 (s, 9H, C_{30-32}),* *2.93 (t, 2H, C_{81}) 2.82 (s, 3H, C_{80}), 2.57 (m, 2H, C_{72}) 2.44 (m, 2H, C_{36}), 2.18 (m, 2H, C_{73}), 2.06 (t, 2H, J= 7.2 Hz, C_{15}), 1.80 (d, 3H, J= 7.1 Hz, C_{71}), 1.44 (m, 3H, C_{67}), 1.11-0.87 (m, 26H, C_{2-14}), 0.72 (t, 3H, J=.7.0 Hz, C_1).* ***^{13}C NMR*** *(101 MHz, DMSO-d6) δ = 189.11 (C=O), 173.04 (C=O), 172.49 (C=O), 171.82 (C=O), 170.71, 169.22, 161.91, 154.41, 149.97, 148.73, 144.57, 141.28, 137.02, 135.71, 135.52, 135.09, 131.88, 128.60, 128.30, 122.63, 121.03, 105.12, 104.23, 96.47, 93.71, 70.82, 65.37, 64.20, 62.65, 62.14, 58.35, 53.06, 52.58, 51.23, 49.35, 45.20, 39.52, 34.74, 34.07, 33.10, 32.46, 31.09, 30.09, 28.75, 28.59, 28.47, 28.42, 28.15, 27.34, 24.12, 22.81, 21.90, 18.20, 17.09, 13.73, 11.71, 11.49, 10.36, 8.52.*

7. NMR characterization of Pyr_3LPC

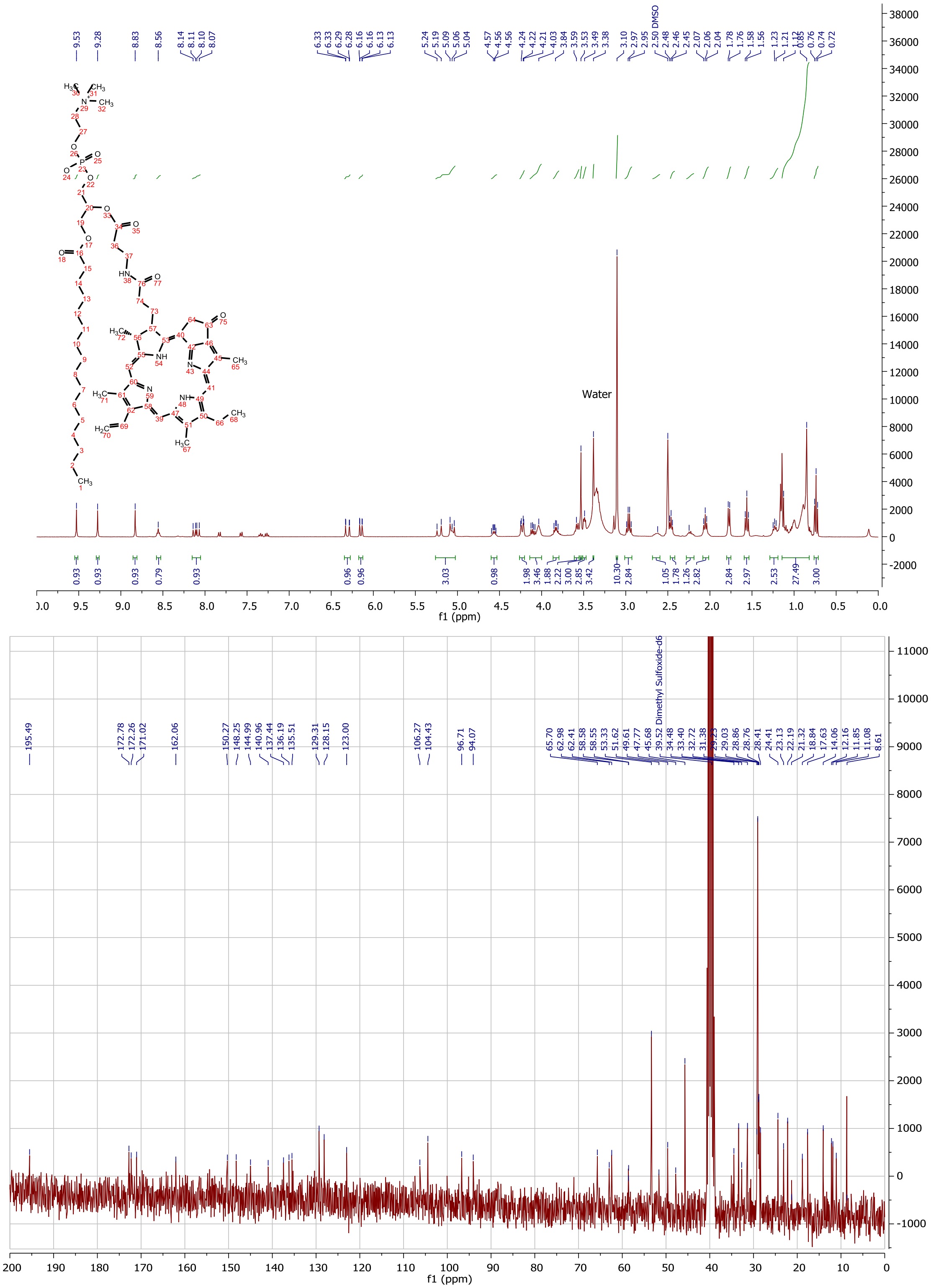

Figure S7. Pyr_3LPC NMR details*:* *^{1}H NMR* *(400 MHz, DMSO-d$_6$) δ (ppm) = 9.53 (s, 1H, C$_{39}$), 9.28 (s, 1H, C$_{41}$), 8.83 (s, 1H, C$_{52}$), 8.56 (m,1H, NH$_{38}$), 8.10 (dd, 1H, J=11.6-17.8 Hz, C$_{69}$), 6.30 (dd, 1H, J= 1.5-17.8 Hz, C$_{70}$), 6.15 (dd, 1H, 1.5-11.6 Hz, C70), 5.21 (d ,1H, J=20 Hz, C$_{64}$), 5.06 (d, 1H, J= 20Hz, C$_{64}$), 5.05 (m, 1H, C$_{20}$), 4.56 (dt, 1H,*

*C_{57}), 4.23 (m, 2H, C_{28}), 4.11 (dd, 1H, C_{56}), 4.03 (m,2H, C_{19}), 3.83 (m, 2H, C_{21}), 3.59 (q, 2H, C_{66}), 3.53 (s, 3H, C_{71}), 3.49 (m, 2H, C_{27}) 3.38 (s, 3H, C_{65}), 3.35 (s, 2H, $_{74}$), 3.10 (s, 12H, C_{30-32}, C_{67}), 2.96 (q, 2H, C_{37}), 2.62 (m, 1H, C_{73}), 2.47 (t, 2H, C_{36}), 2.25 (m, 1H, C_{73}), 2.06 (m, 2H, C_{15}), 1.77 (d, 3H, C_{72}), 1.56 (d, 3H, C_{68}), 1.22-0.83 (m, 26H, C_{2-14}), 0.73 (t, 3H, C_{1}). **^{13}C NMR** (75 MHz, DMSO) δ 195.49 (C=O), 172.78(C=O), 172.26(C=O), 171.02 (C=O), 162.06, 150.27, 148.25, 144.99, 140.96, 137.44, 136.19, 135.51, 129.31, 128.15, 123.00, 106.27, 104.43, 96.71, 94.07, 65.70, 62.98, 62.41, 58.58, 58.55, 53.33, 51.62, 49.61, 47.77, 45.68, 39.52, 34.48, 33.40, 32.72, 31.38, 29.23, 29.03, 28.86, 28.76, 28.41, 24.41, 23.13, 22.19, 21.32, 18.84, 17.63, 14.06, 12.16, 11.85, 11.08, 8.61.*

8. NMR characterization of Ph_4LPC

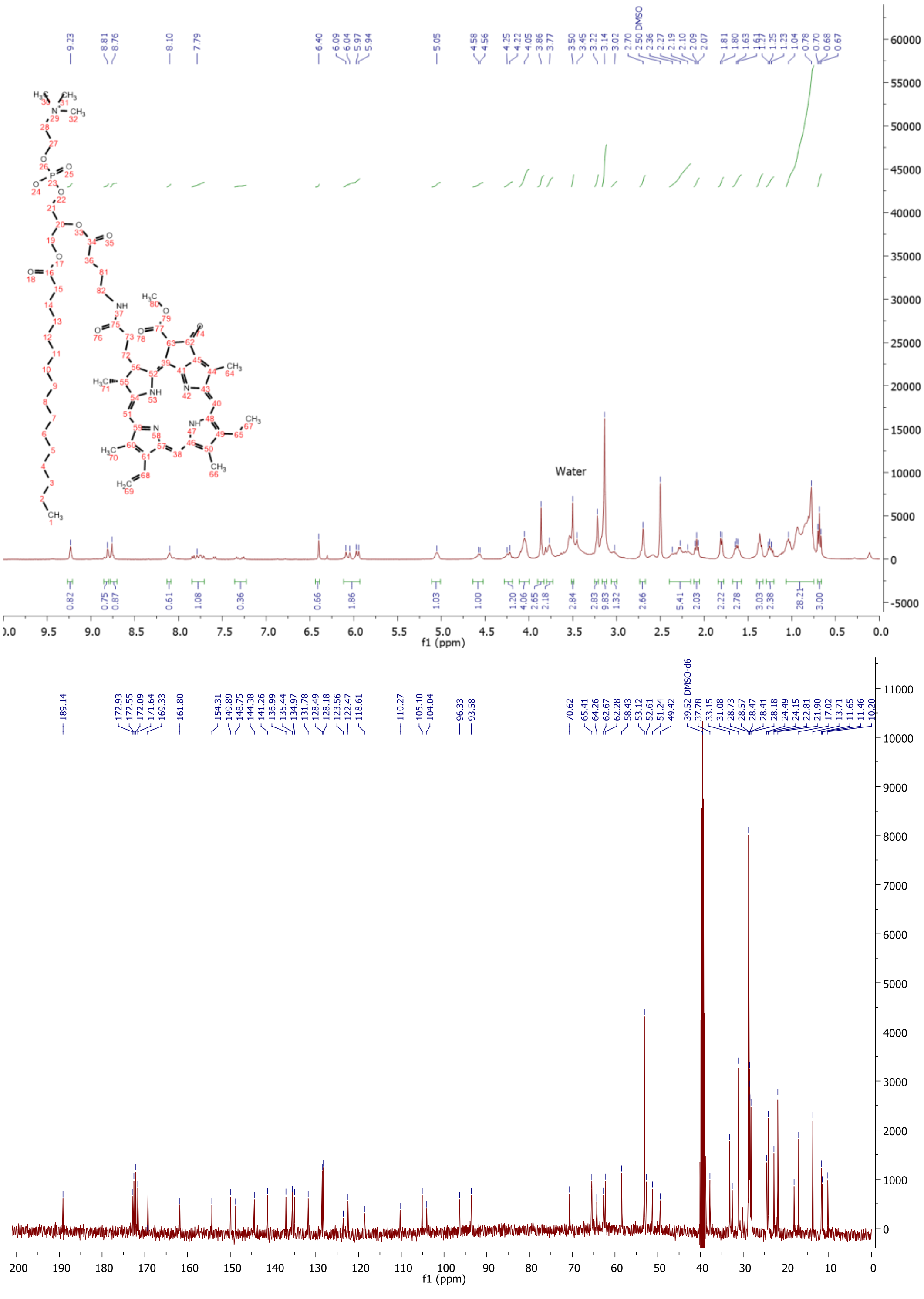

Figure S8. Ph_4LPC NMR details: ^{1}*H NMR* *(400 MHz, DMSO-d_6) δ (ppm) = 9.23 (s, 1H, C_{38}), 8.81 (1H, s, C_{40}), 8.76 (s, 1H, C_{51}), 8.10 (s, 1H, NH_{37}), 7.84-7.72 (dd, 1H, J= 11.6-17.7 Hz, C_{68}), 6.40 (s, 1H, NH_{47}), 6.09-6.04 (dd, 1H, J=1.3-18 Hz, C_{69}), 5.97-5.94 (dd, 1H, J=1.3-11.5 Hz, C_{69}), 5.05 (m, 1H, C_{20}), 4.58 (m, 1H, C_{63}), 4.22 (m, 2x1H, C_{55}-C_{56}) , 4.05 (m, 4H, C_{19}-C_{28}), 3.86 (s, 3H, C_{70}), 3.77 (m, 2H, C_{21}), 3.60 (m, 2H, C_{65}), 3.45 (m, 2H, C_{27}), 3.50 (s,* *3H, C_{64}), 3.22 (s, 3H, C_{66}), 3.14 (s, 9H, C_{30-32}), 2.70 (s, 3H, C_{80}), 2.36-2.18 (m, 6H, C_{36}-C_{82}-C_{73}), 2.10 (2H, t, J=7.1 Hz, C_{15}), 1.80 (d, 3H, J= 5.2 Hz, C_{71}) , 1.63 (m, 2H, C_{81}), 1.38 (t, 3H, J= 7.1 Hz, C_{67}), 1.04-0.78 (m, 28H, C_{2-14}), 0.68 (t, 3H, J=7.1 Hz, C_1), -2.15 (bs, 1H, NH_{53}).* ***^{13}C NMR*** *(101 MHz, DMSO) δ = 189.14 (C=O), 172.93 (C=O), 172.55 (C=O), 172.09 (C=O), 171.64, 169.33, 161.80, 154.31, 149.89, 148.75, 144.38, 141.26, 136.99, 135.44, 134.97, 131.78, 128.49, 128.18, 123.56, 122.47, 118.61, 110.27, 105.10, 104.04, 96.33, 93.58, 70.62, 65.41, 64.26, 62.67, 62.28, 58.43, 53.12, 52.61, 51.24, 49.42, 39.52, 37.78, 33.15, 32.57, 31.08, 28.73, 28.57, 28.47, 28.41, 28.18, 24.49, 24.15, 22.81, 21.90, 18.10, 17.02, 13.71, 11.65, 11.46, 10.20.*

9. NMR characterization of Pyr$_4$LPC

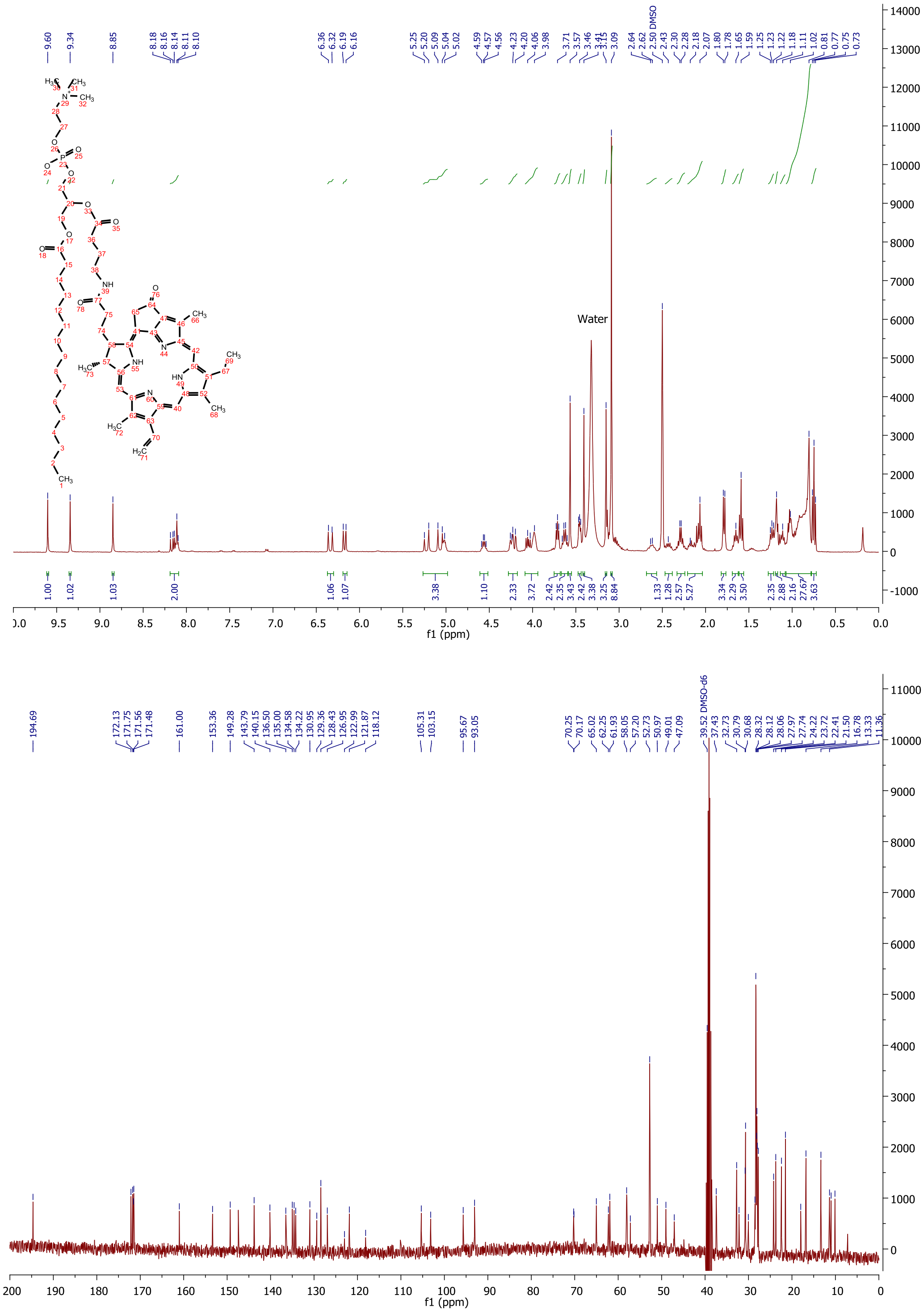

Figure S9. Pyr$_4$LPC NMR details: ***^{1}H NMR*** *(400 MHz DMSO-d$_6$) δ (ppm) = 9.64 (s, 1H, C_{40}), 9.36 (s, 1H, C_{42}), 8.85 (s, 1H, C_{53}), 8.53 (m,1H, NH_{39}), 8.15 (dd, 1H, J=11.6-17.8 Hz, C_{70}), 6.34 (dd, 1H, J= 1.5-17.8 Hz, C_{71}), 6.17 (dd, 1H, 1.5-11.6 Hz, C_{71}), 5.25-5.03 (d ,1H, J=20 Hz, C_{65}), 5.11-5.06 (d, 1H, J= 20Hz, C_{65}), 5.03 (m, 1H, C_{20}), 4.58 (dt, 1H, C_{56}), 4.26 (m, 2H, C_{28}), 4.10 (dd, 1H, C_{57}), 4.04 (m,2H, C_{19}), 3.77 (m, 2H, C_{21}), 3.66 (q, 2H, C_{67}), 3.57 (s, 3H, C_{72}), 3.51 (m, 2H, C_{27}), 3.41 (s, 3H, C_{66}), 3.16 (s, 3H, C_{68}), 3.12 (s, 11H, C_{31-33}, C_{75}), 2.64 (m, 1H, C_{74}), 2.43 (m,* *2H, C_{38}), 2.30 (m, 2H, C_{36}), 2.18 (m, 1H, C_{74}), 2.07 (m, 2H, C_{15}), 1.79 (d, 3H, C_{73}), 1.65 (m, 2H, C_{37}), 1.59 (t, 2H, C_{69}), 1.25-0.8 (m, 26H, C_{2-13}), 0.75 (t, 3H, C_1). **^{13}C NMR** (101 MHz, DMSO) δ = 194.69 (C=O), 172.13 (C=O), 171.75 (C=O), 171.56, 171.48, 161.00, 153.36, 149.28, 143.79, 140.15, 136.50, 135.00, 134.58, 134.22, 130.95, 129.36, 128.43, 126.95, 122.99, 121.87, 118.12, 105.31, 103.15, 95.67, 93.05, 70.25, 70.17, 65.02, 62.25, 61.93, 58.05, 57.20, 52.73, 50.97, 49.01, 47.09, 39.52, 37.43, 32.73, 32.19, 30.79, 30.68, 30.05, 28.51, 28.32, 28.12, 28.06, 27.97, 27.74, 24.22, 23.72, 22.41, 21.50, 17.97, 16.78, 13.33, 11.36, 10.98, 10.10.*

10. Absorbance and fluorescence spectra of Ph_2LPC and Pyr_2LPC assemblies

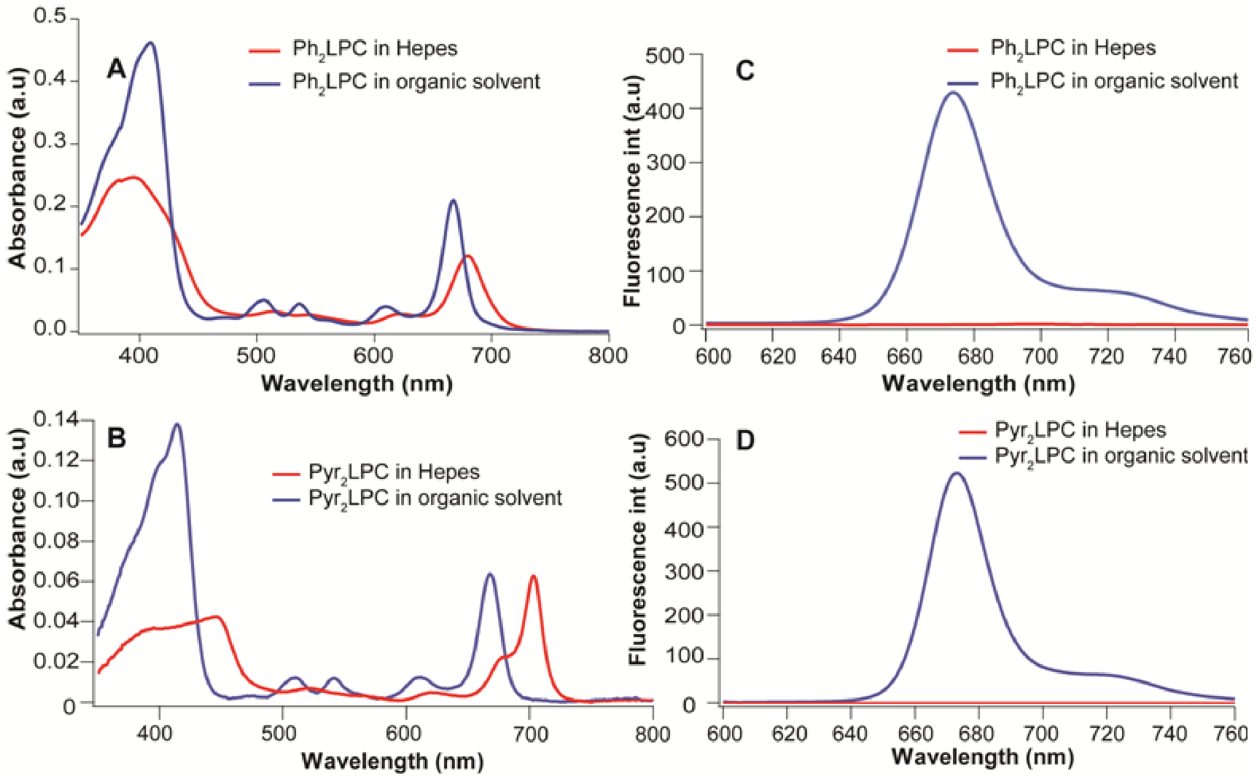

Figure S10. Absorbance and fluorescence spectra of Ph_2LPC-DSPE-PEG_{2000} (A, C) and Pyr_2LPC-DSPE-PEG_{2000} (B, D) assemblies, before (red line) and after (blue line) their solubilization in HEPES/MeOH/THF (0.2, 0.8, 1 mL) mixture. The theoretical PS concentration is 25 µM.

11. Absorbance and fluorescence spectra of Ph_4LPC and Pyr_4LPC assemblies

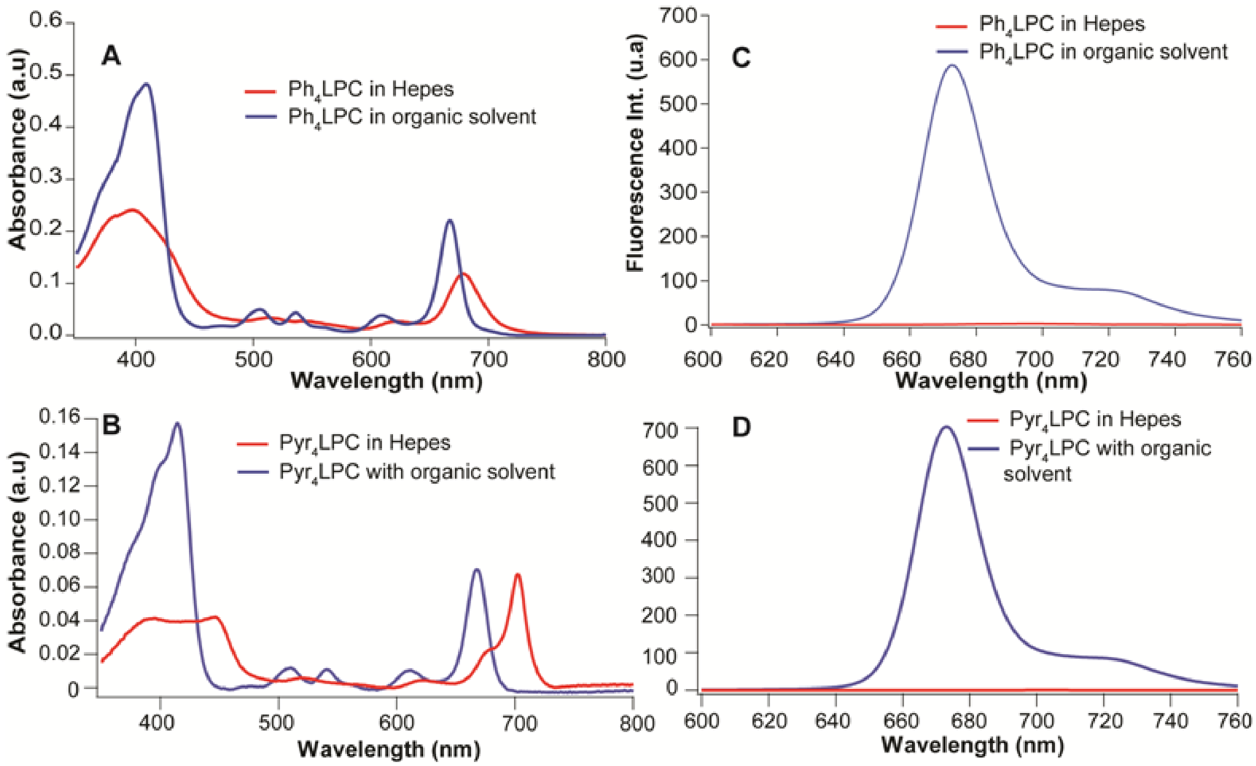

Figure S11. Absorbance and fluorescence spectra of Ph_4LPC-DSPE-PEG_{2000} (A, C) and Pyr_4LPC-DSPE-PEG_{2000} (B, D) assemblies, before (red line) and after (blue line) their solubilization in HEPES/MeOH/THF (0.2, 0.8, 1 mL) mixture. The theoretical PS concentration is 25 µM.

12. DSC heating scans for DPPC lamellar suspensions incorporating either Pheo a or Pyro a

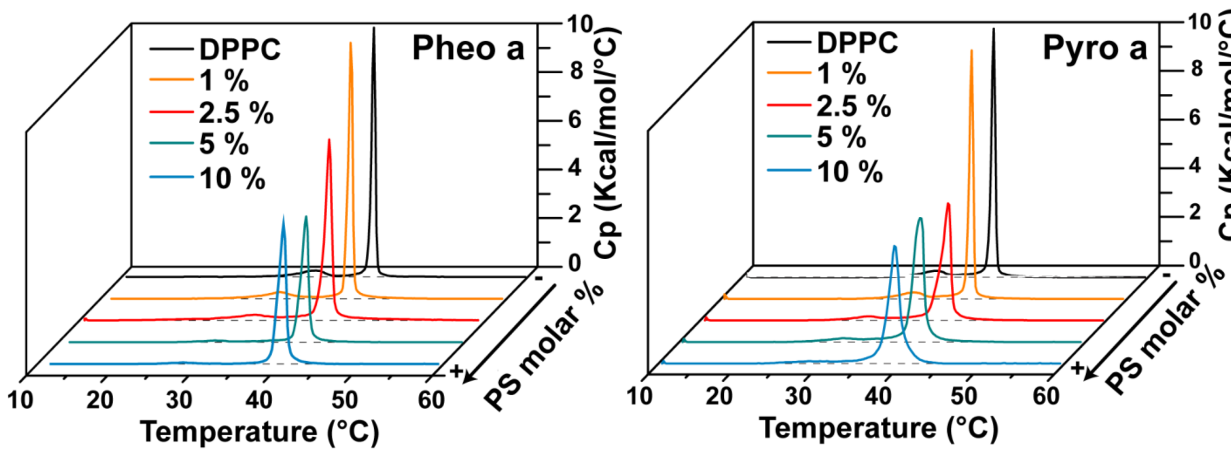

Figure S12. DSC heating scans for DPPC lamellar suspensions incorporating increasing molar percentages (1-10 mol %) of Pheo a (left column) or Pyro a (right column).

13. Fluorescence spectra of DPPC liposomes incorporating either Ph_2LPC or Pyr_2LPC

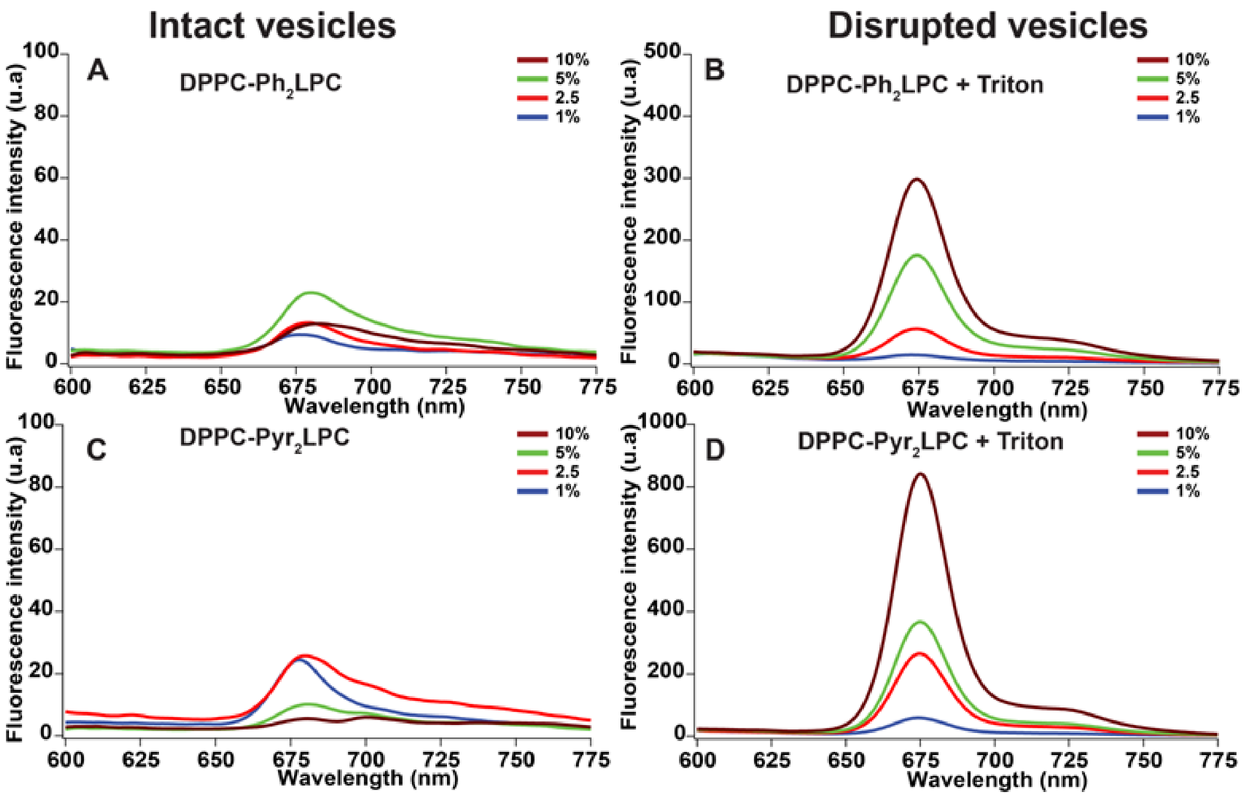

Figure S13. Fluorescence spectra of DPPC liposomes incorporating different molar percentage (1-10 mol %) of either Ph_2LPC (A, B) or Pyr_2LPC (C, D), before (A, C) and after (B, D) their disruption by adding Triton X-100 (1 % V/V).

14. Fluorescence spectra of DPPC liposomes incorporating either Ph_3LPC or Pyr_3LPC

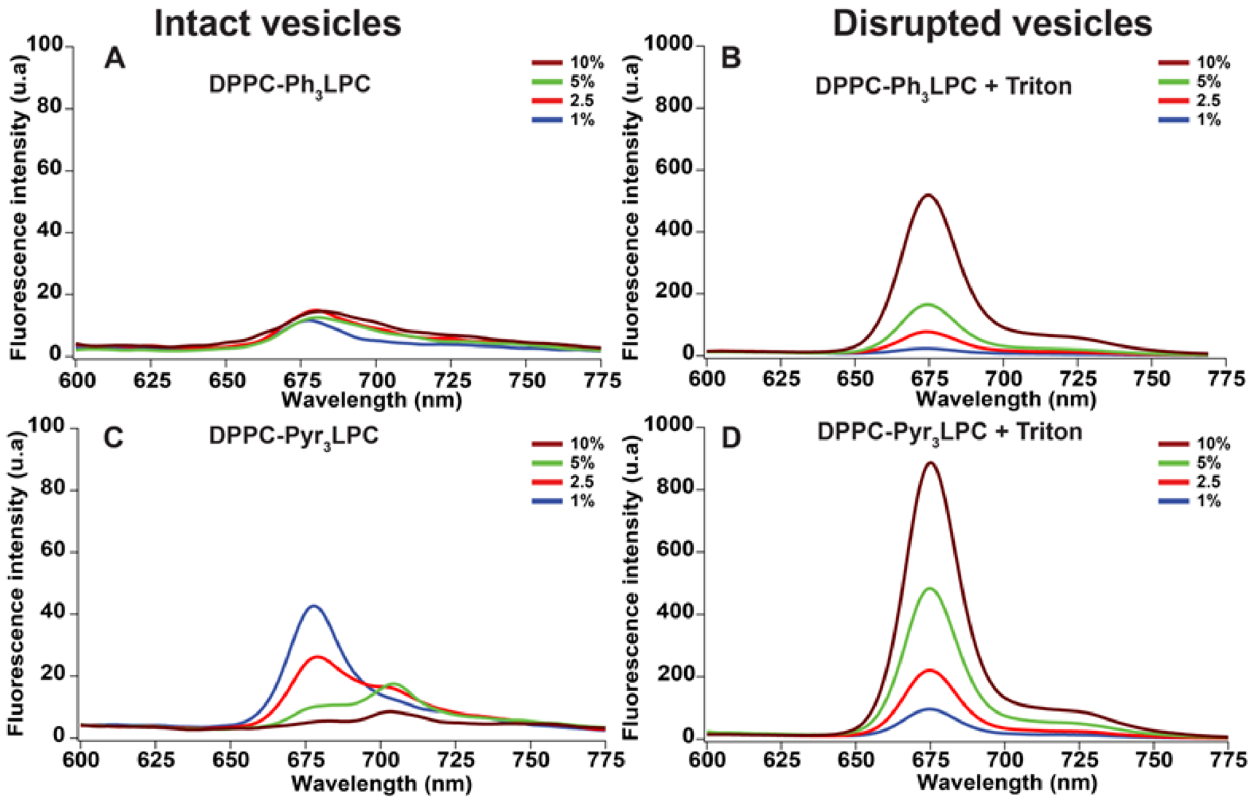

Figure S14. Fluorescence spectra of DPPC liposomes incorporating different molar percentage (1-10 mol %) of either Ph_3LPC (A, B) or Pyr_3LPC (C, D), before (A, C) and after (B, D) their disruption by adding Triton X-100 (1 % V/V).

15. Fluorescence spectra of DPPC liposomes incorporating either Ph_4LPC or Pyr_4LPC

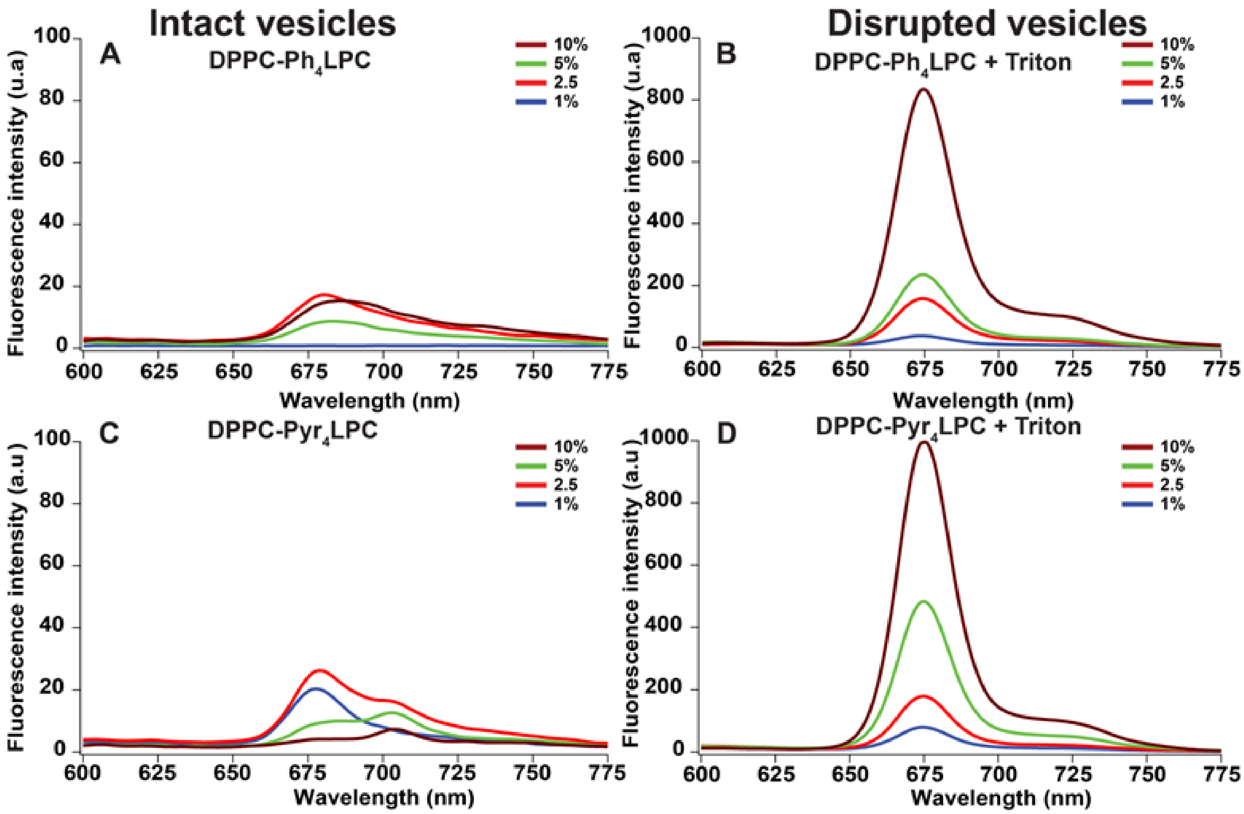

Figure S15. Fluorescence spectra of DPPC liposomes incorporating different molar percentage (1-10 mol %) of either Ph_4LPC (A, B) or Pyr_4LPC (C, D), before (A, C) and after (B, D) their disruption by adding Triton X-100 (1 % V/V).

16. Absorbance spectra of DPPC liposomes incorporating either Ph_2LPC or Pyr_2LPC

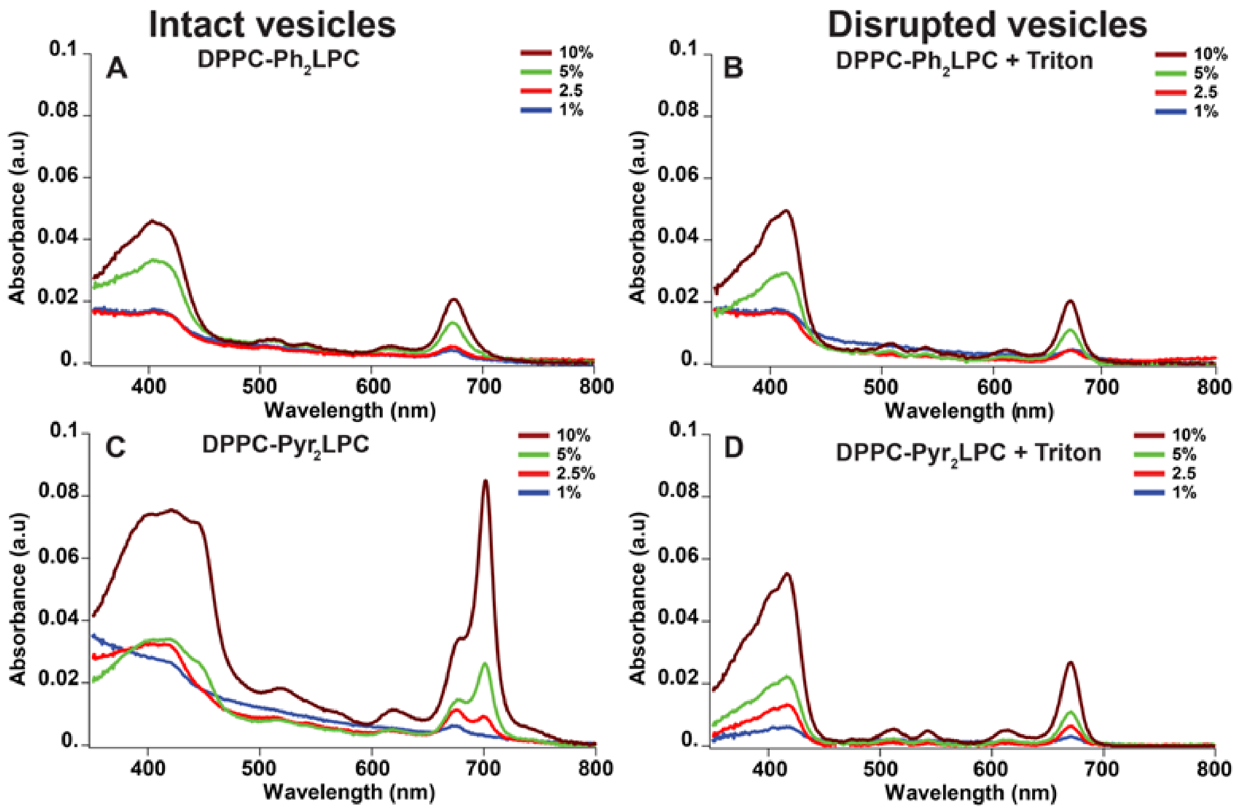

Figure S16. Absorbance spectra of DPPC liposomes incorporating different molar percentage (1-10 mol %) of either Ph_2LPC (A, B) or Pyr_2LPC (C, D), before (A, C) and after (B, D) their disruption by adding Triton X-100 (1 % V/V).

17. Absorbance spectra of DPPC liposomes incorporating either Ph_4LPC or Pyr_4LPC

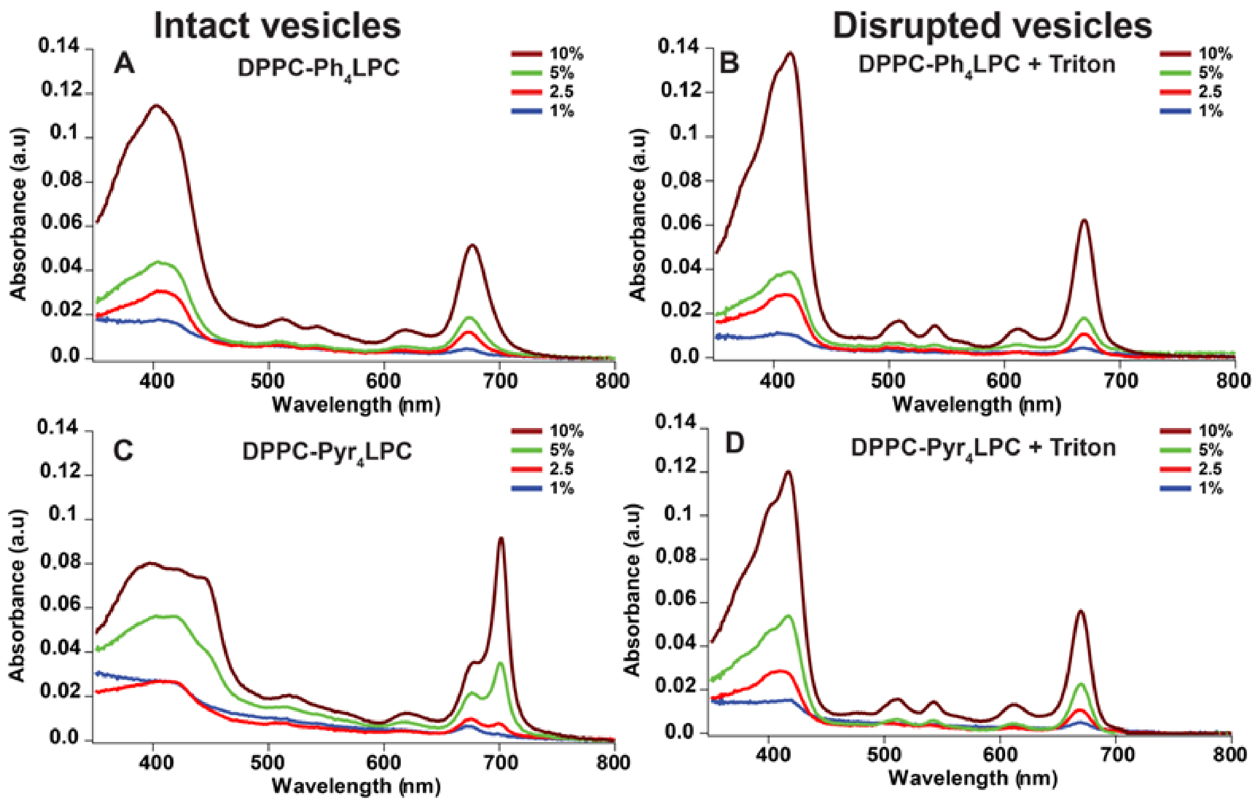

Figure S17. Absorbance spectra of DPPC liposomes incorporating different molar percentage (1-10 mol %) of either Ph_4LPC (A, B) or Pyr_4LPC (C, D), before (A, C) and after (B, D) their disruption by adding Triton X-100 (1 % V/V).

18. Absorbance spectra of POPC liposomes incorporation Pyr_xLPC at 10 mol %

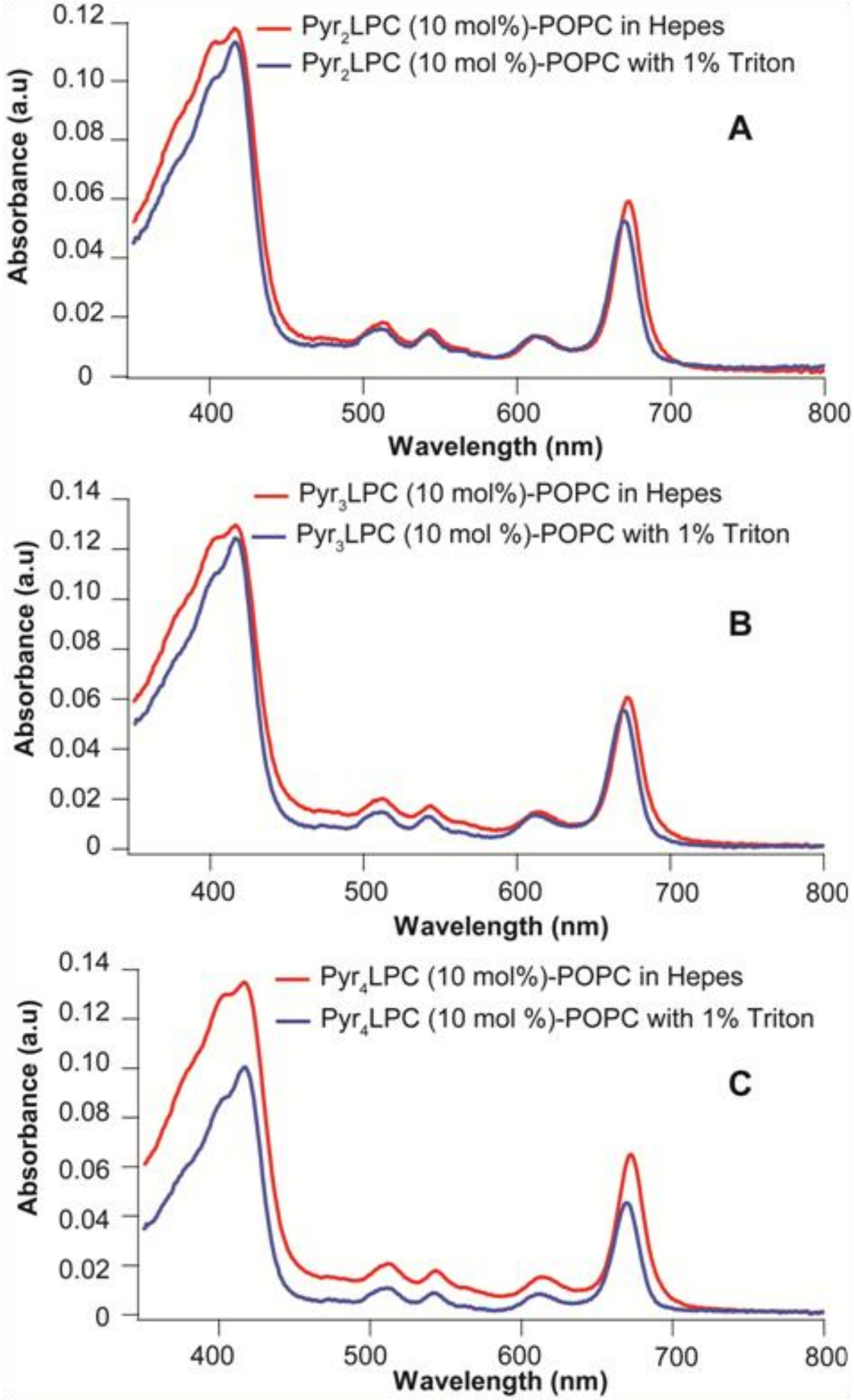

Figure S18. Absorption spectra of POPC bilayers incorporated in 10mol % of Pyr_2LPC (A), Pyr_3LPC (B) and Pyr_4LPC (C) before and after their rupture in the presence of detergent.

19. Cryo-electron micrographs of POPC vesicles incorporating

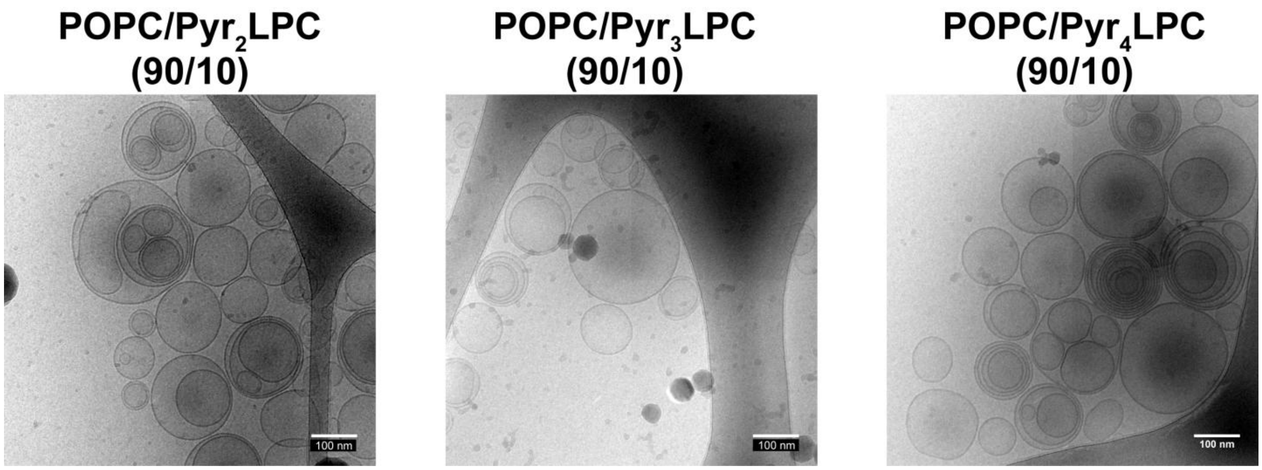

Figure S19. Cryo-electron micrographs of POPC vesicles incorporating 10 mol % of Pyr_xLPC conjugates in HEPES buffer.

20. Absorbance spectra of DPPC, DSPC and DAPC liposomes incorporating Pyr_3LPC

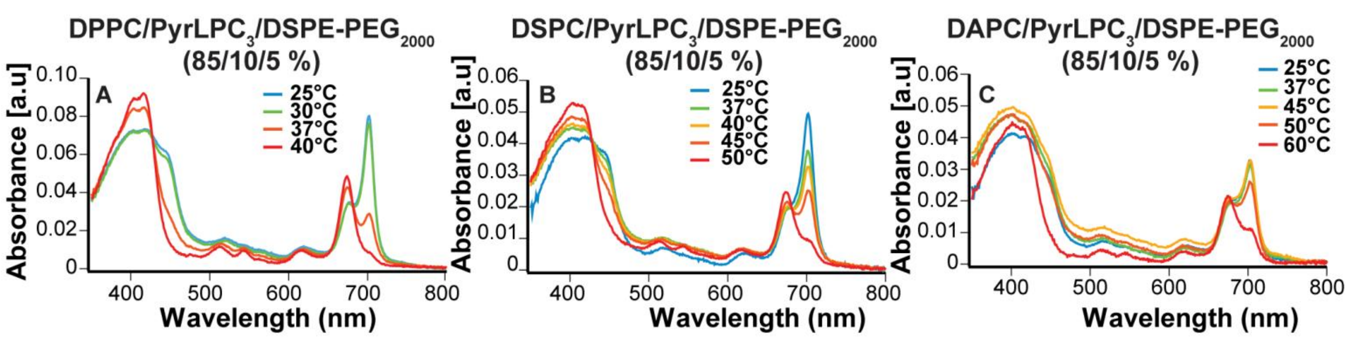

Figure S20. Absorption spectra of (A) DPPC, (B) DSPC and (C) DAPC liposomes doped with 10 mol% of Pyr_3LPC and 5 mol% of DSPE-PEG_{2000}.

21. Calculated area per lipid deduced from MD simulations for Pyr_xLPC and Ph_xLPC

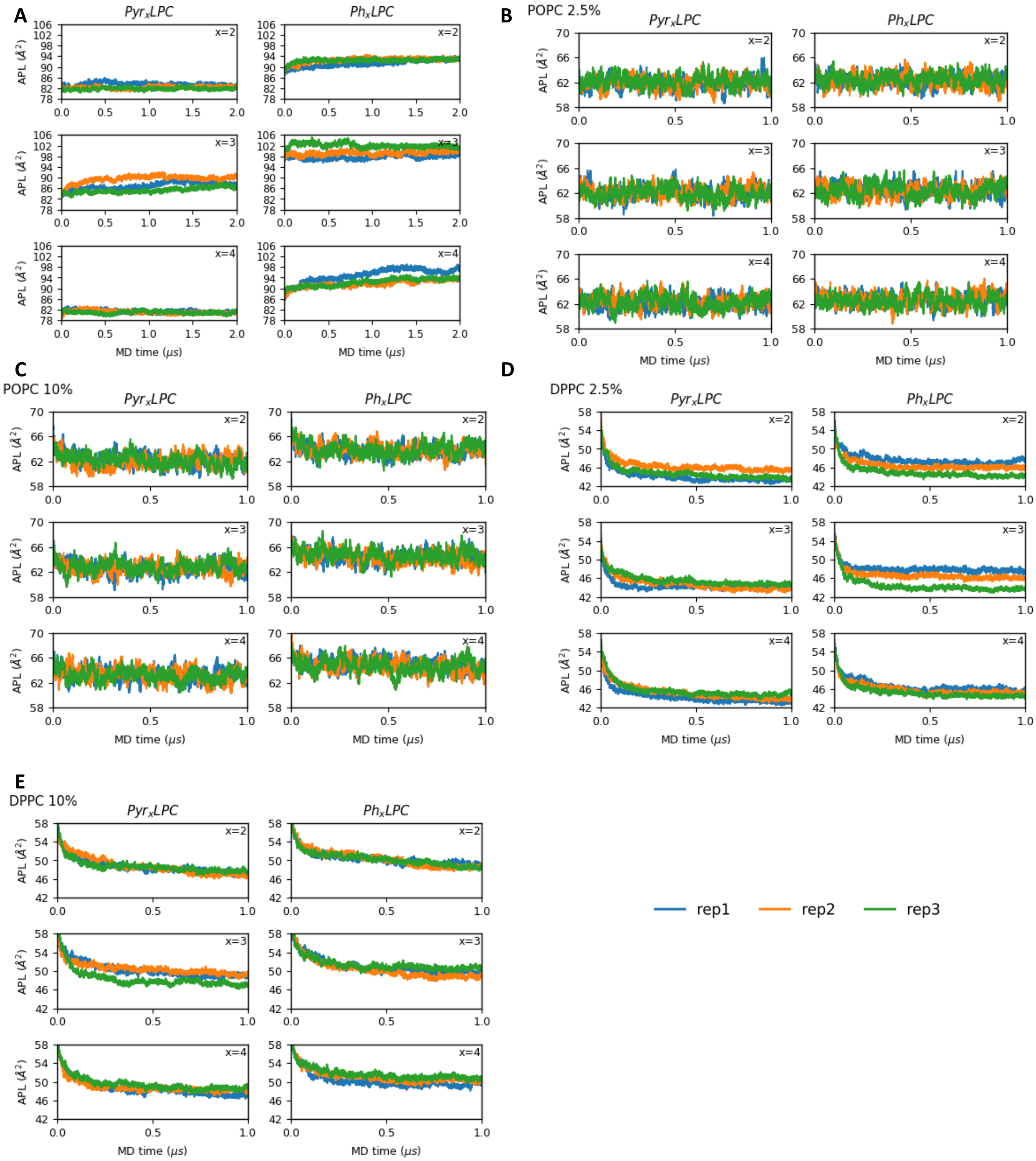

Figure S21. Calculated area per lipid along MD simulations for Pyr_xLPC and Ph_xLPC in (A) pure LPC systems, (B) POPC 2.5 mol%, (C) POPC 10 mol %, (D) DPPC 2.5mol % and (E) DPPC 10mol %.

22. Calculated PC polar head P-atom density profiles for pure Pyr$_x$LPC, Ph$_x$LPC and their mixtures with either POPC or DPPC

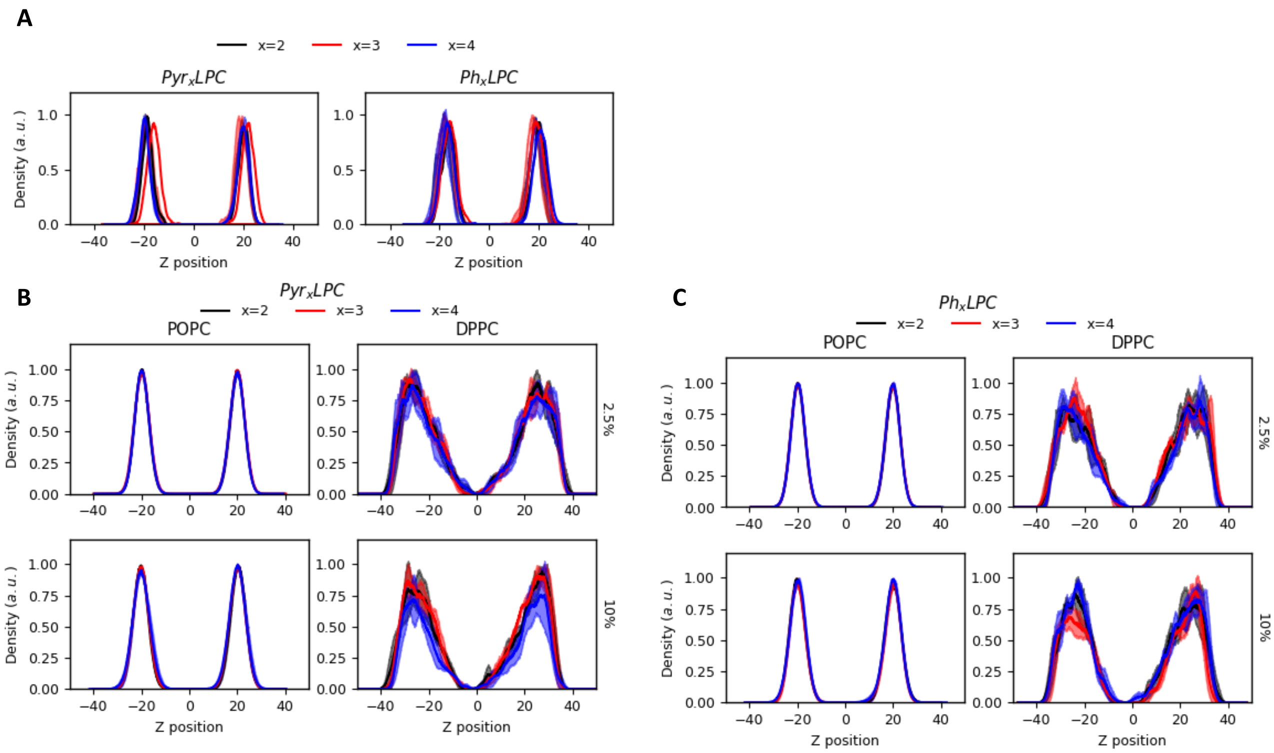

Figure S22. Calculated PC polar head P-atom density profiles for (A) pure Pyr$_x$LPC and Ph$_x$LPC, (B) POPC- and DPPC-Pyr$_x$LPC mixtures, and (C) POPC- and DPPC-Ph$_x$LPC mixtures.

23. Calculated thicknessess maps for pure Pyr_xLPC, Ph_xLPC and their mixtures with either POPC or DPPC

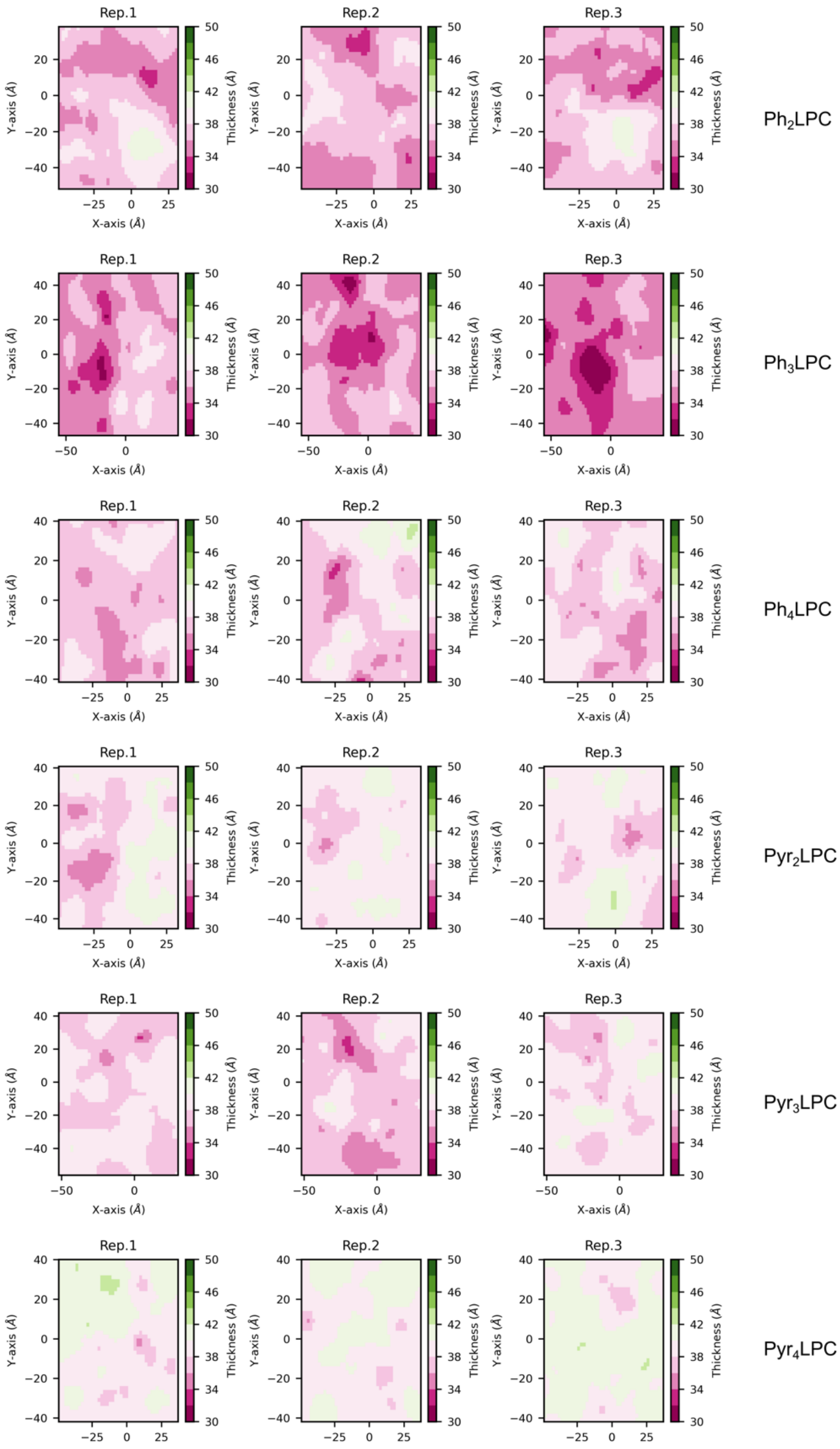

Figure S23. Calculated thickness maps for pure Ph_xLPC and Pyr_xLPC.

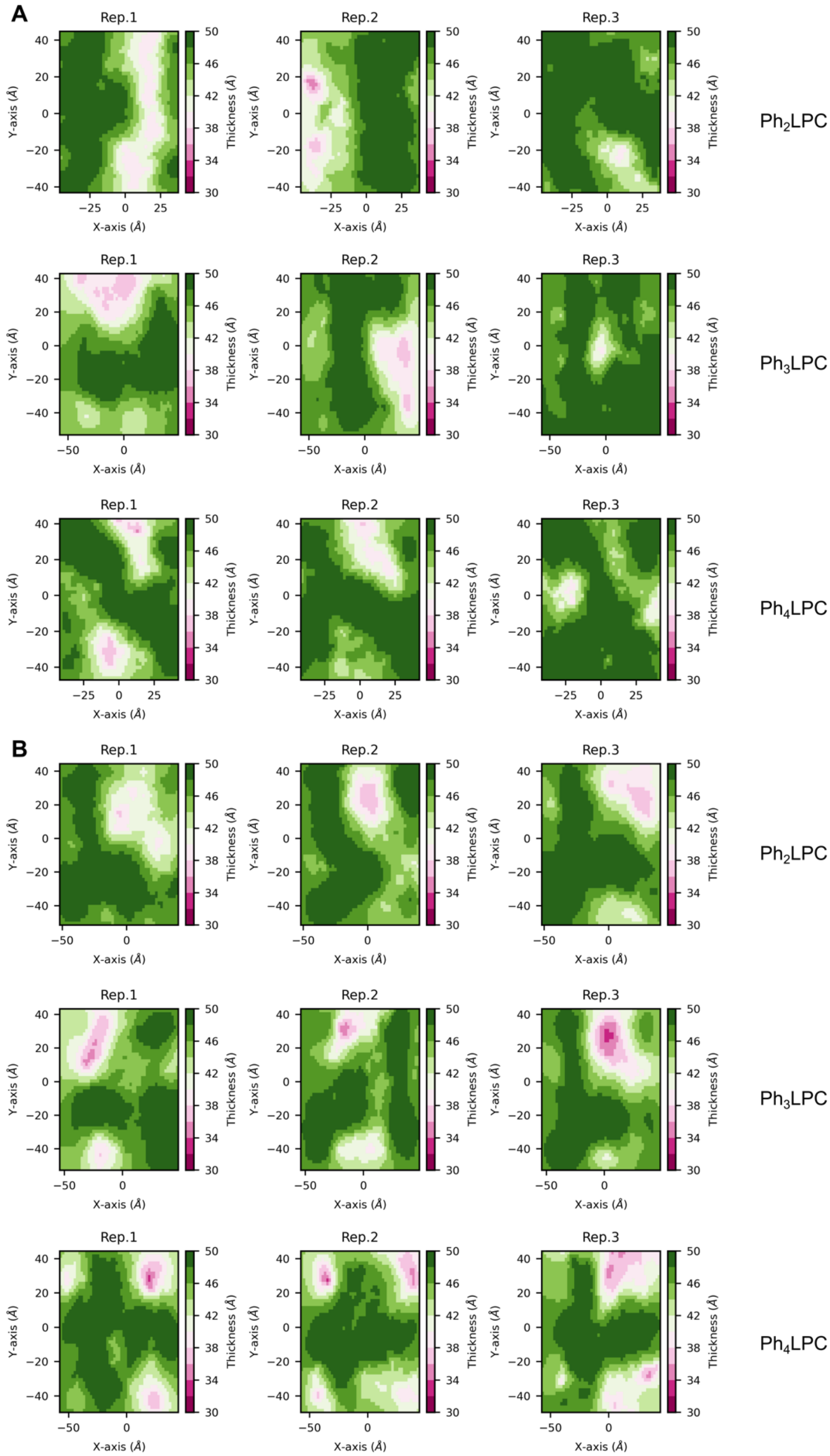

Figure S24. Calculated thickness maps for DPPC-Ph$_x$LPC mixtures at (A) 2.5 mol % and (B) 10 mol %.

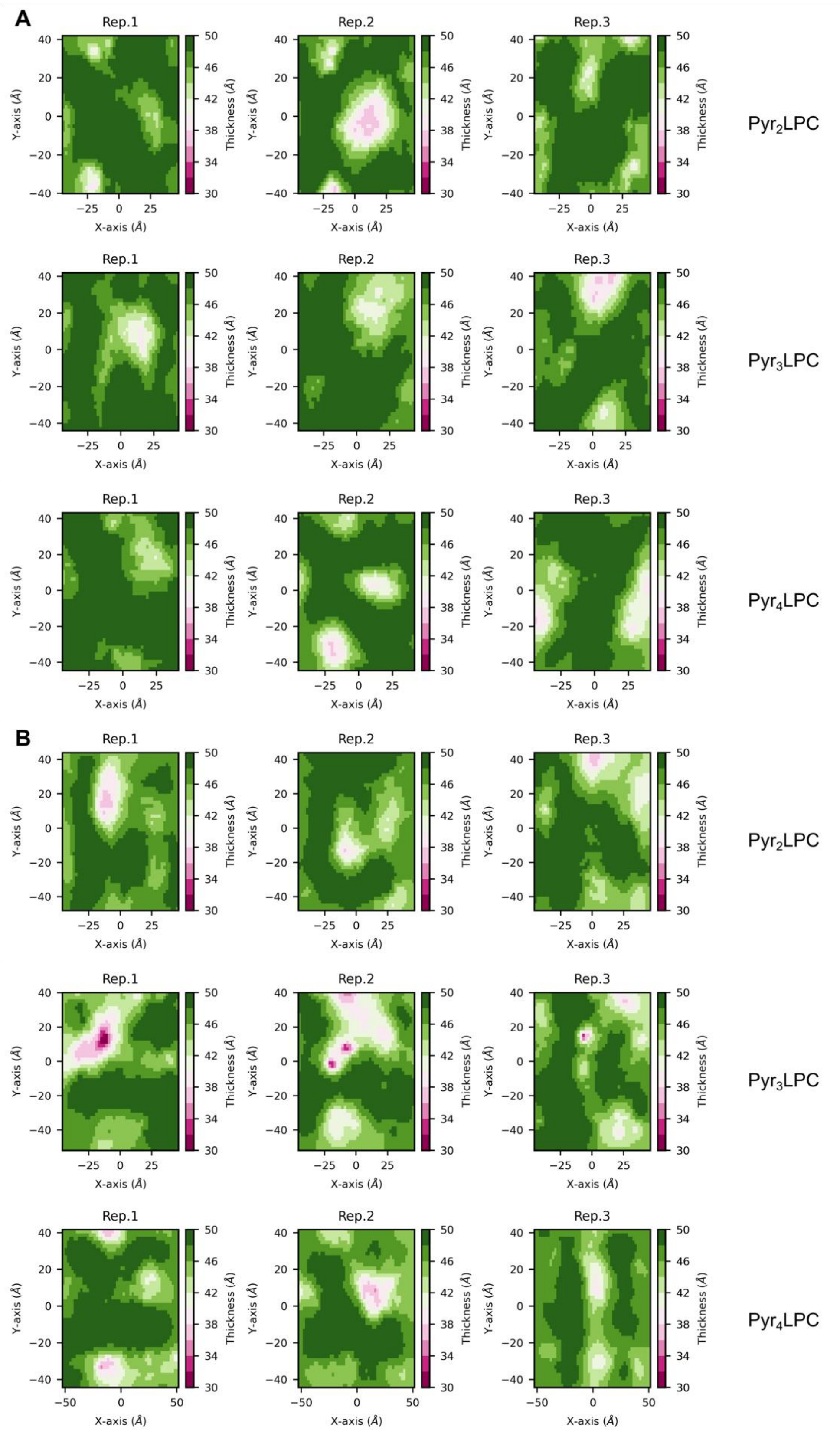

Figure S25. Calculated thickness maps for DPPC-Pyr$_x$LPC mixtures at (A) 2.5 mol % and (B) 10 mol %.

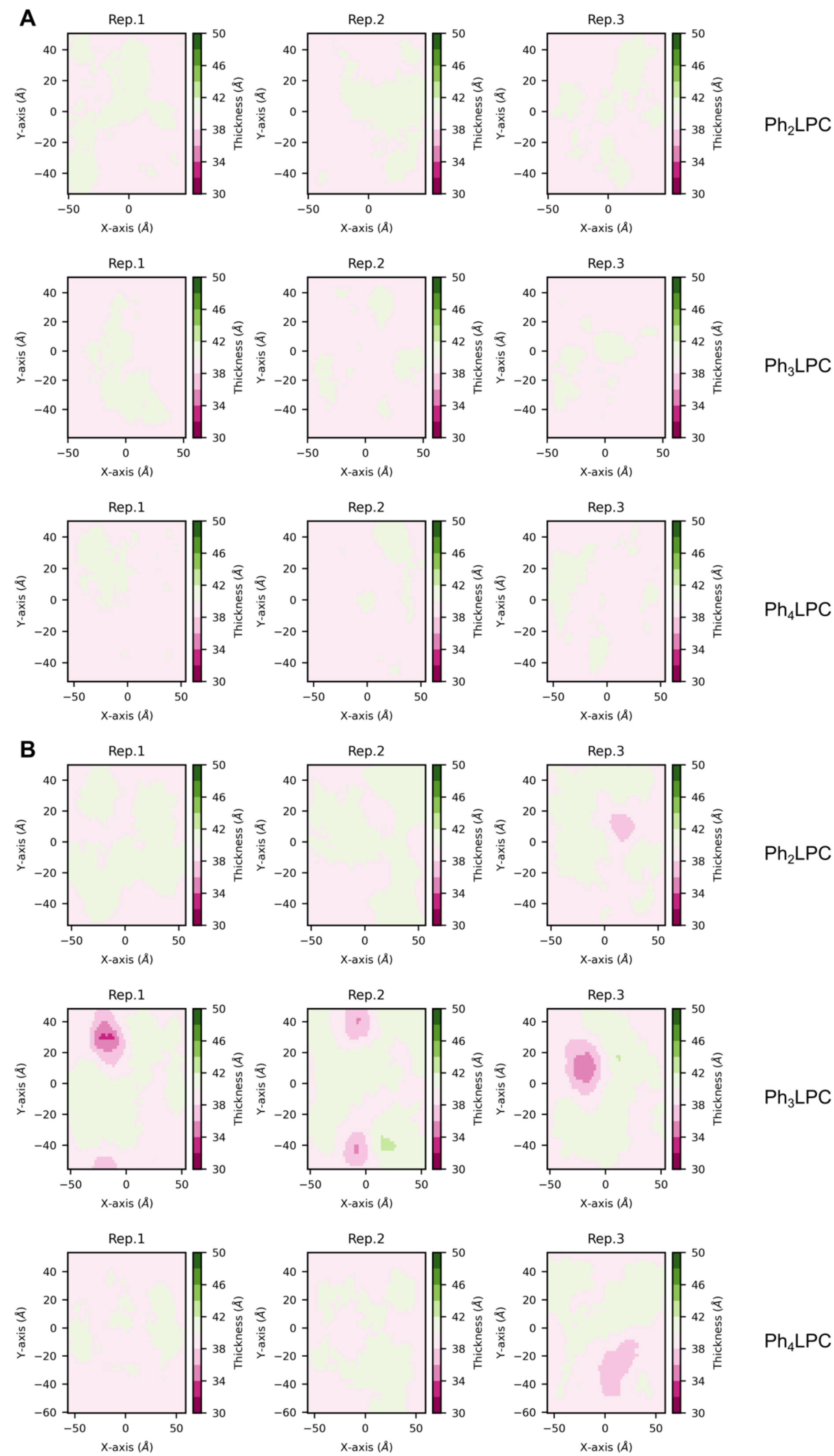

Figure S26. Calculated thickness maps for POPC-Ph$_x$LPC mixtures at (A) 2.5 mol % and (B) 10 mol %.

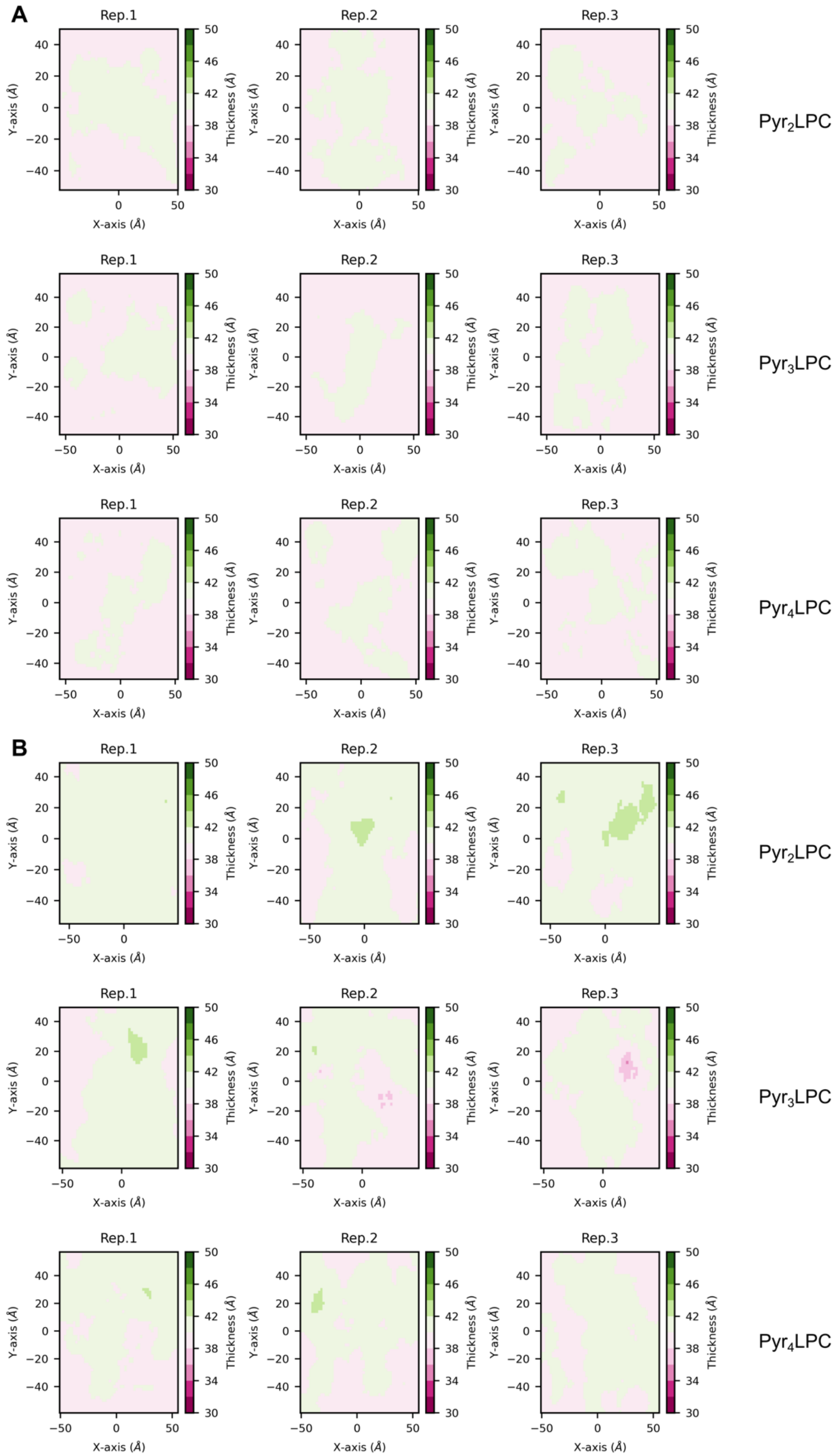

Figure S27. Calculated thickness maps for POPC-Ph$_x$LPC mixtures at (A) 2.5 mol % and (B) 10 mol %.

24. Lipid order of sn_1 lipid tail of Pyr_xLPC and Ph_xLPC in pure Pl-Por bilayers

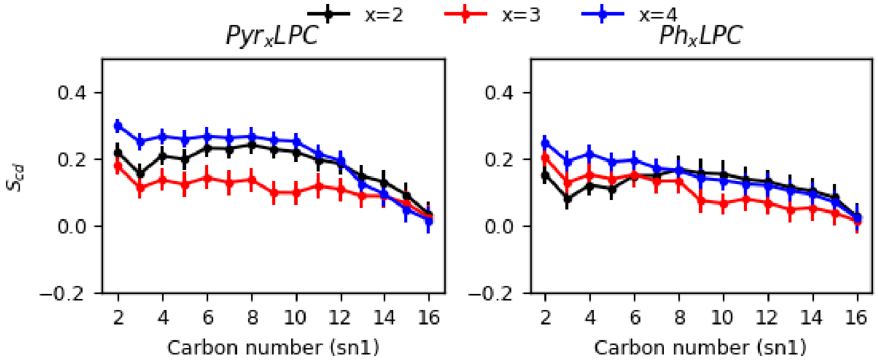

Figure S28. Lipid order of sn_1 lipid tail of Pyr_xLPC and Ph_xLPC calculated in pure Pl-Por bilayers.

25. Lipid order of sn_1 lipid tail of Pyr_xLPC and Ph_xLPC when incorporated in either DPPC or POPC lipid bilayers

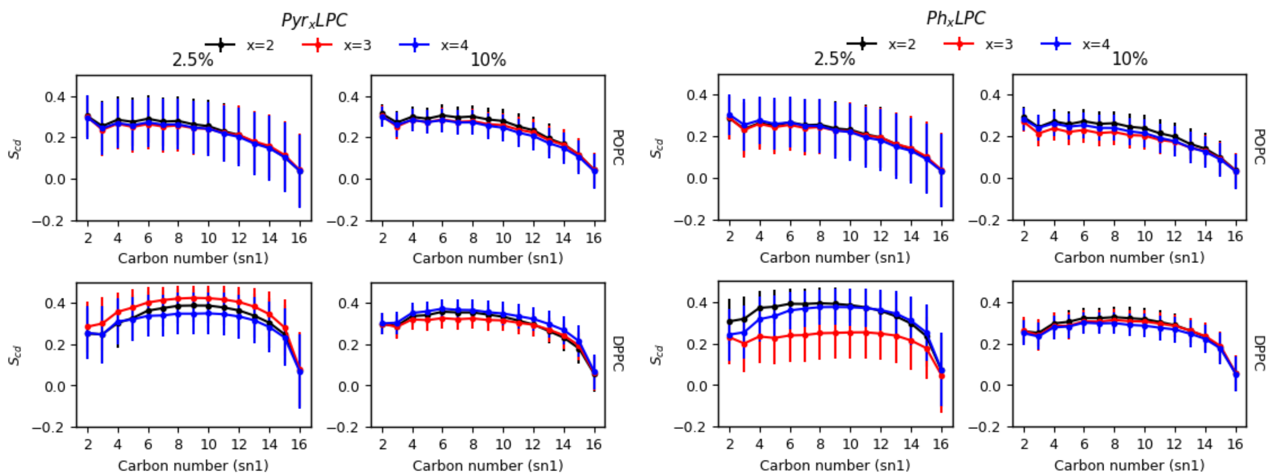

Figure S29. Lipid order of sn_1 lipid tail of Pyr_xLPC (left) and Ph_xLPC (right) calculated in DPPC and POPC lipid bilayers doped with differet Pl-Por conjuates.

26. Lipid order of sn1 and sn2 lipid tails for Pyr_xLPC and Ph_xLPC when incorporated in either DPPC or POPC lipid bilayers

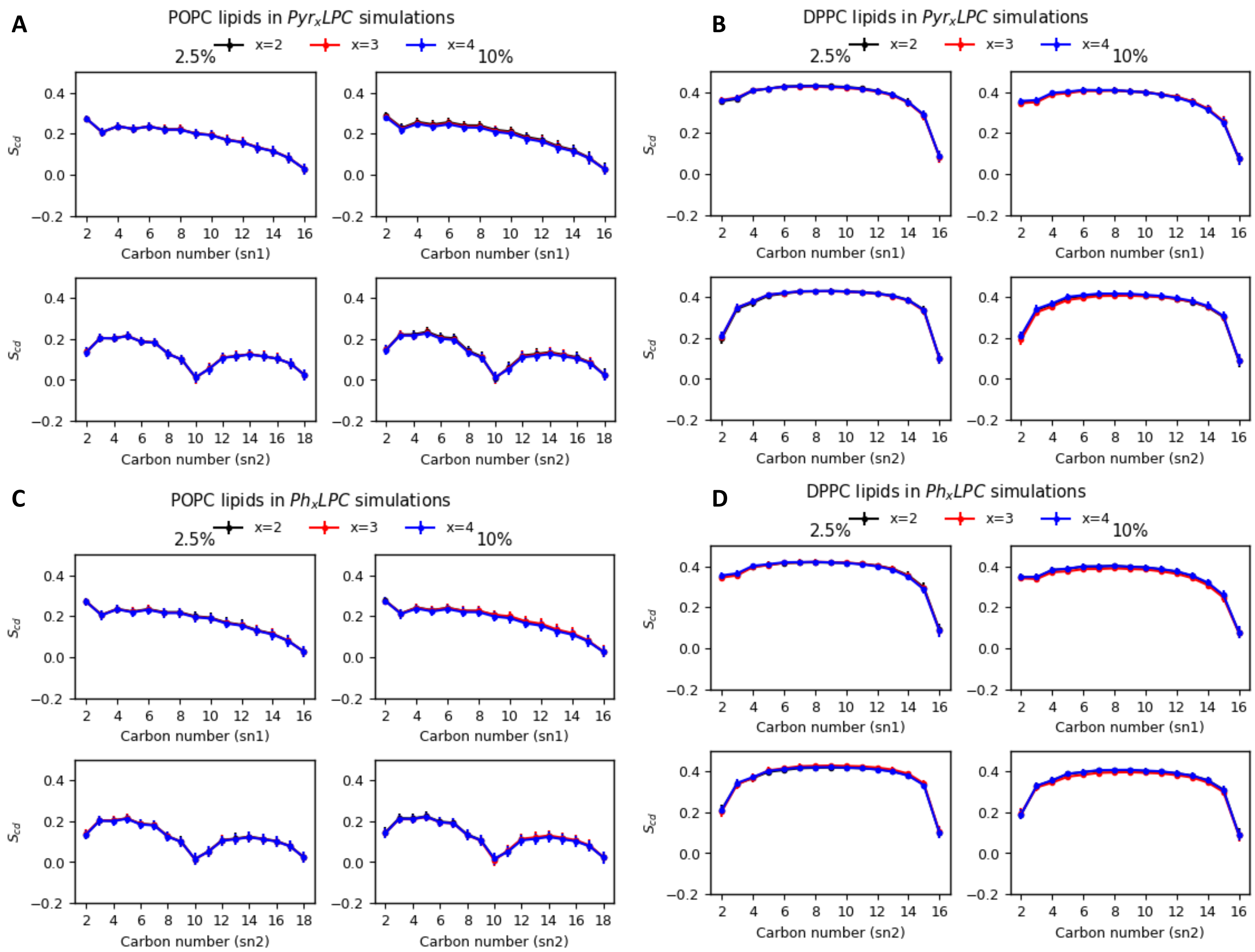

Figure S30. Lipid order of sn1 and sn2 lipid tails for (A) POPC-Pyr_xLPC, (B) DPPC-Pyr_xLPC, (C) POPC-Ph_xLPC and (D) DPPC-Ph_xLPC systems.

27. Normalized order parameters for porphyrin core normal vector in different bilayer systems

A

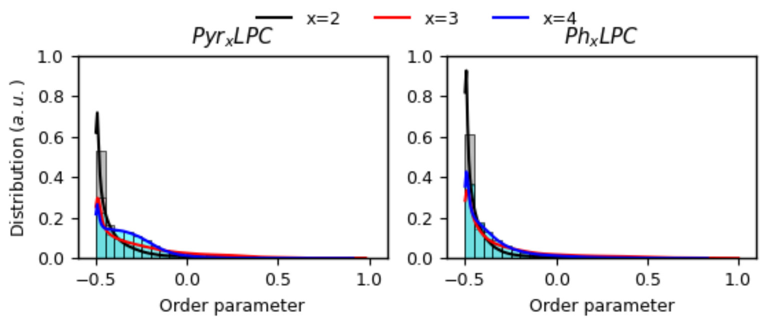

B

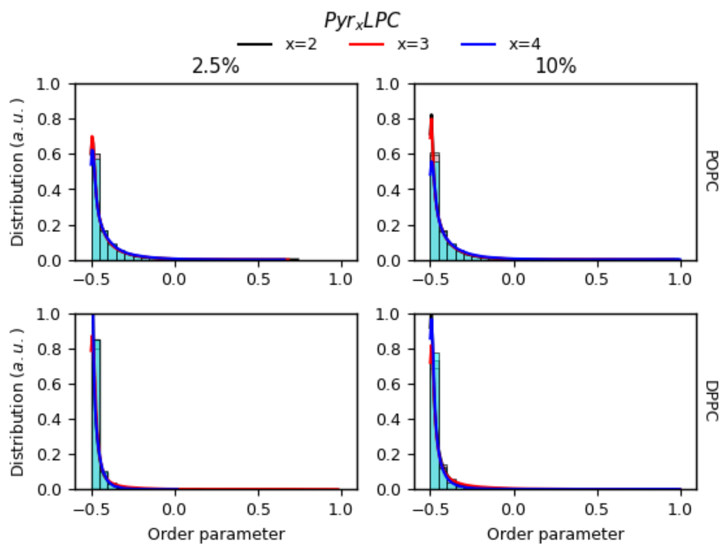

C

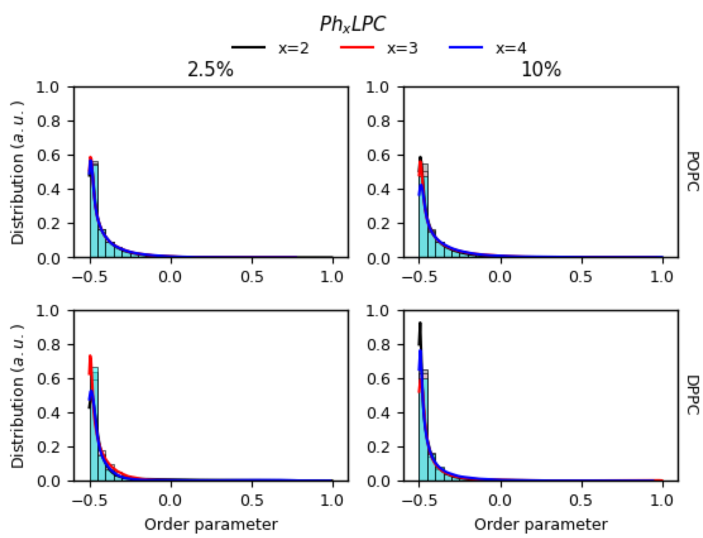

Figure S31. Normalized order parameters for porphyrin core normal vector in (A) pure Pyr$_x$LPC and Ph$_x$LPC simulations, (B) DPPC- and POPC-Pyr$_x$LPC mixtures, and (C) DPPC- and POPC-Ph$_x$LPC mixtures

28. Distributions of z-projected distances between porphyrin cores and the center-of-mass of lipid bilayer membranes

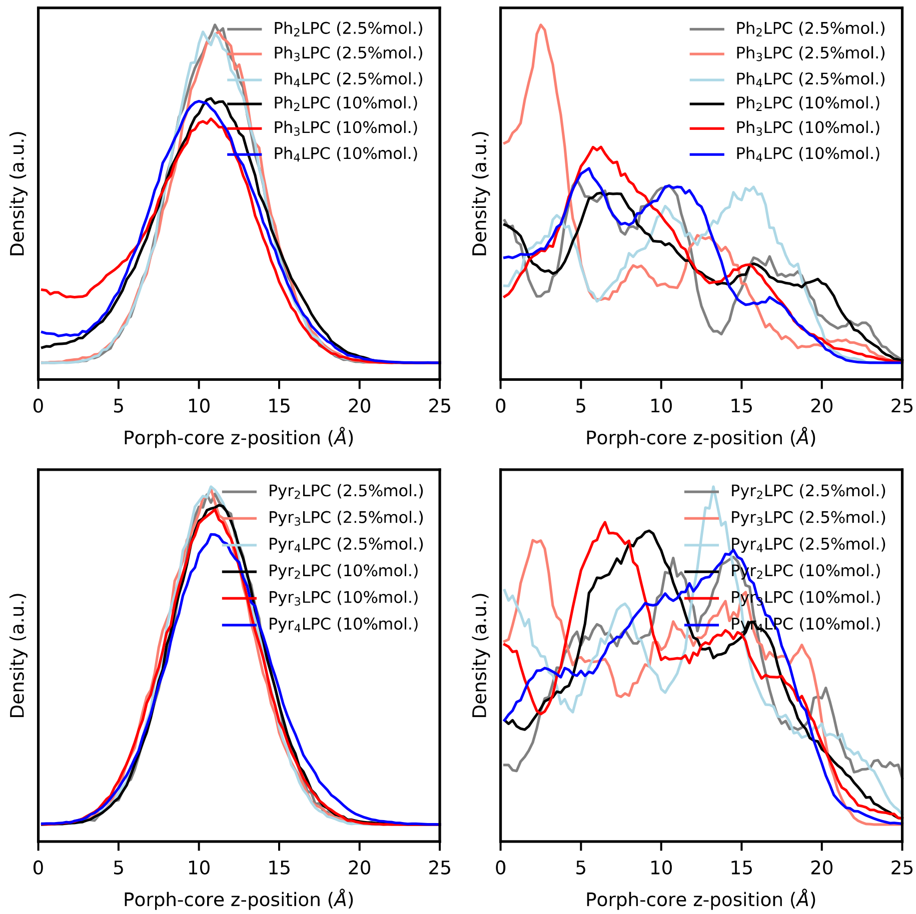

Figure S32. Distributions of z-projected distances between porphyrin cores and the center-of-mass of lipid bilayer membranes for Ph_xLPC (top) and Pyr_xLPC (bottom) systems in DPPC (left) and POPC (right) lipid bilayer membranes.

29. π-Stacking events in the different systems

Table S1. π-Stacking events in the different systems, including overall fractions for both inter-leaflet π-stacking events and all events, as well as the number of different pair of porphyrin dimers.

			Ph_XLPC				Pyr_XLPC			
			Inter leaflet	all	%	N	Inter leaflet	all	%	N
POPC	2.50%	x=2	0.000	0.004	0.0%	1	-	-	-	0
		x=3	-	-	-	0	0.000	0.052	0.0%	1
		x=4	0.000	0.033	0.0%	1	-	-	-	0
	10%	x=2	0.271	2.132	12.7%	31	-	0.693	0.0%	26
		x=3	1.834	3.121	58.8%	27	-	1.263	0.0%	29
		x=4	0.317	0.953	33.3%	22	-	0.778	0.0%	22
DPPC	2.50%	x=2	0.000	0.012	0.0%	1	-	-	-	0
		x=3	0.561	0.561	100.0%	2	-	-	-	0
		x=4	-	-	-	0	-	-	-	0
	10%	x=2	0.494	2.049	24.1%	17	0.000	0.512	0.0%	11
		x=3	1.736	2.391	72.6%	10	0.590	1.117	52.8%	12
		x=4	0.469	1.788	26.2%	14	0.000	0.093	0.0%	2
Pure Pl-Por		x=2	27.635	50.292	54.9%	262	56.822	89.728	63.3%	294
		x=3	26.456	33.782	78.3%	134	32.949	46.158	71.4%	177
		x=4	20.434	35.053	58.3%	246	38.924	82.498	47.2%	377